Published in final edited form as:
Sci Signal. ; 6(303): ra102. doi:10.1126/scisignal.2004373.

The ζ Isoform of Diacylglycerol Kinase Plays a Predominant Role in Regulatory T Cell Development and TCR-Mediated Ras Signaling

Rohan P. Joshi[1], **Amanda M. Schmidt**[2], **Jayajit Das**[3], **Dariusz Pytel**[1], **Matthew J. Riese**[1], **Melissa Lester**[1], **J. Alan Diehl**[1], **Edward M. Behrens**[4], **Taku Kambayashi**[2], and **Gary A. Koretzky**[1,5,*,†]

[1]Abramson Family Cancer Research Institute, Perelman School of Medicine, University of Pennsylvania, Philadelphia, PA 19104, USA

[2]Department of Pathology and Laboratory Medicine, Perelman School of Medicine, University of Pennsylvania, Philadelphia, PA 19104, USA

[3]Battelle Center for Mathematical Medicine, The Research Institute at the Nationwide Children's Hospital, and Departments of Pediatrics, Physics, and Biophysics, The Ohio State University, Columbus, OH 43205, USA

[4]The Children's Hospital of Philadelphia, Philadelphia, PA 19104, USA

[5]Department of Medicine, Perelman School of Medicine, University of Pennsylvania, Philadelphia, PA 19104, USA

Abstract

Diacylglycerol (DAG) is a critical second messenger that mediates T cell receptor (TCR)–stimulated signaling. The abundance of DAG is reduced by the diacylglycerol kinases (DGKs), which catalyze the conversion of DAG to phosphatidic acid (PA) and thus inhibit DAG-mediated signaling. In T cells, the predominant DGK isoforms are DGKα and DGKζ, and deletion of the genes encoding either isoform enhances DAG-mediated signaling. We found that DGKζ, but not DGKα, suppressed the development of natural regulatory T (T_{reg}) cells and predominantly mediated Ras and Akt signaling downstream of the TCR. The differential functions of DGKα and DGKζ were not attributable to differences in protein abundance in T cells or in their localization to the contact sites between T cells and antigen-presenting cells. RasGRP1, a key DAG-mediated activator of Ras signaling, associated to a greater extent with DGKζ than with DGKα; however, in silico modeling of TCR-stimulated Ras activation suggested that a difference in RasGRP1 binding

*Corresponding author. koretzky@mail.med.upenn.edu.
†Present address: Department of Medicine, Weill Cornell Medical College, New York, NY 10065, USA.

Author contributions: R.P.J. conceived, designed, and performed most experiments and wrote the paper; A.M.S. performed experiments and provided stimulating discussion under the mentor-ship of T.K.; J.D. performed computational studies and provided stimulating discussion; D.P. aided with experimental design and provided stimulating discussion under the mentorship of J.A.D.; M.J.R. aided with experimental design and provided stimulating discussion; M.L. aided with experimental design; E.M.B. and T.K. provided stimulating discussion; and G.A.K. conceived and supervised the work, designed experiments, and wrote the paper.

Competing interests: The authors declare that they have no competing interests.

affinity was not sufficient to cause differences in the functions of each DGK isoform. Rather, the model suggested that a greater catalytic rate for DGKζ than for DGKα might lead to DGKζ exhibiting increased suppression of Ras-mediated signals compared to DGKα. Consistent with this notion, experimental studies demonstrated that DGKζ was more effective than DGKα at catalyzing the metabolism of DAG to PA after TCR stimulation. The enhanced effective enzymatic production of PA by DGKζ is therefore one possible mechanism underlying the dominant functions of DGKζ in modulating T_{reg} cell development.

INTRODUCTION

T cell activation requires engagement of the T cell receptor (TCR) with peptide presented by major histocompatibility complex (MHC) proteins on the surface of antigen-presenting cells (APCs), which leads to the production of second messengers that activate pathways critical for the normal development, activation, differentiation, and proliferation of T cells. At the interface between the T cell and the APC, which is termed the immunological synapse, TCR engagement leads to the formation of a multimolecular complex that recruits and activates phospholipase C–γ1 (PLC-γ1) (1–3). PLC-γ1 hydrolyzes phosphatidylinositol 4,5-bisphosphate (PIP_2) to form cytosolic inositol 1,4,5-trisphosphate (IP_3) and membrane-diffusible diacylglycerol (DAG), second messengers that are critical for T cell activation. DAG is essential for the activation of diverse downstream signaling cascades, including the Ras, nuclear factor κB (NF-κB), and Akt pathways, which are integrated with other key signals to promote T cell effector function (4–7). The concentration of DAG therefore must be finely tuned through not only its production but also its metabolism for appropriate control of a T cell response.

Diacylglycerol kinases (DGKs) are a family of 10 enzymes in mice and humans that catalyze the phosphorylation of DAG to form phosphatidic acid (PA), and they share common catalytic and C1 domains. T cells have large amounts of the α and ζ isoforms of DGK in addition to the d isoform, whose function in lymphocytes remains unknown. Deletion of the genes encoding DGKα or DGKζ in mice results in T cells with enhanced activation of Ras and extracellular signal–regulated kinase (ERK) in response to TCR engagement (8–10). In addition, both DGKα and DGKζ regulate the T cell effector response to pathogens in mice (11). These data suggest that DGKα and DGKζ have overlapping roles in T cells. Consistent with this notion, simultaneous deletion of the genes encoding DGKα and DGKζ in mice reveals a severe defect in thymocyte development that is not seen in mice deficient in either DGKα or DGKζ alone, suggesting a redundant function for these molecules in T cell development.

DGKα and DGKζ have distinct domain architectures that suggest differential regulation of these molecules, perhaps directing isoform-specific functions in addition to their redundant roles. DGKα contains a Ca^{2+}-responsive EF-hand regulatory domain that modulates its kinase activity in vitro and its membrane translocation in Jurkat cells (a human $CD4^+$ T cell leukemia cell line) (12–16). DGKζ contains a myristoylated, alanine-rich protein kinase C substrate (MARCKS) domain, phosphorylation of which may modulate its kinase activity in vitro and its localization in Jurkat cells (17–19), together with ankyrin and PDZ-binding

domains that mediate interactions with other proteins. In Jurkat cells, DGKζ is the predominant regulator of DAG after TCR engagement, which suggests that this isoform has specific functions (18). No direct investigation of the relative roles of DGKα and DGKζ in primary T cells has been performed, although differences in the functions of DGKα and DGKζ in TCR signaling have been suggested previously (9). Furthermore, whether isoform-specific functions exist in vivo is unknown.

Here, we showed that DGKζ has dominant roles over DGKα, in the development of regulatory T (T_{reg}) cells and in TCR signaling in primary T cells. Loss of DGKζ, but not of DGKα, enhanced the development of thymic T_{reg} cells. DGKζ also exhibited quantitatively greater control over signaling downstream of Ras after TCR engagement than did DGKα. Overexpression of DGKα did not rescue the suppression of TCR signaling in DGKζ-deficient T cells, suggesting a nonredundant role for DGKζ in controlling TCR signaling. However, these differences in function were not a result of the decreased abundance of endogenous DGKα protein or of differences in the gross localization of DGKα and DGKζ to the immunological synapse. In addition, although DGKζ demonstrated a greater ability to form a complex with Ras guanyl nucleotide–releasing protein 1 (RasGRP1), in silico studies suggested that changes in RasGRP1 binding alone would not lead to functional differences in the activation of Ras signaling by either DGK isoform. Rather, in silico data suggested that DGKζ would predominantly control Ras signaling in T cells if DGKζ had a greater catalytic activity than that of DGKα. This prediction was consistent with experimental data demonstrating that DGKζ had enhanced effective enzymatic activity, or ability to produce PA after TCR stimulation, relative to DGKα. Our findings therefore suggest that DGKζ plays a selective role in the suppression of T_{reg} cell development and a predominant role in the suppression of DAG-mediated Ras signaling, in part because of its greater effective enzymatic activity compared to that of DGKα.

RESULTS

DGKζ, but not DGKα, suppresses the development of natural T_{reg} cells

Deletion of *Dgkz* results in the enhanced development of natural T_{reg} (nT_{reg}) cells (20). To determine whether DGKα similarly suppressed the development of this cell lineage during thymocyte maturation, we examined the proportion of thymic $FoxP3^+$ cells within the pool of CD4 single-positive (CD4 SP) T cells of wild-type, DGKα-deficient, and DGKζ-deficient mice (Fig. 1). The percentages of CD4 SP thymocytes were similar for mice of all genotypes (fig. S1). As reported by Schmidt *et al*. (20), we found that mice deficient in DGKζ had increased percentages of thymic $FoxP3^+$ cells and $CD25^+FoxP3^-$ cells, a population enriched for T_{reg} cell precursors, compared to wild-type mice (Fig. 1, A to C). In contrast, mice deficient in DGKα showed no such increase in the percentage of $FoxP3^+$ cells in the thymus and had an intermediate number of $CD25^+FoxP3^-$ cells. The percentages of splenic $FoxP3^+$ cells were also increased only by deficiency in DGKζ, and not DGKα (Fig. 1, D and E). These data suggest that DGKζ is distinct in its ability to suppress the development of nT_{reg} cells, and that it has functions in vivo that are distinct from those of DGKα.

DGKζ exhibits greater quantitative control than does DGKα over TCR-stimulated ERK phosphorylation

TCR signaling is critical for the development of nT_{reg} cells and the activation of T cells. Both DGKα and DGKζ suppress DAG-mediated signaling after TCR engagement (8, 9, 18), but a direct comparison of the role of DGKα and DGKζ in primary T cells has not yet been performed. We predicted that differences in the ability of DGKα and DGKζ to regulate TCR signaling might mirror the observed differences in their functions in vivo, such that DGKζ would exhibit greater control over DAG-mediated TCR signaling than would DGKα. To test this possibility, we examined the phosphorylation of ERK in T cells after TCR stimulation, an assay used previously to examine modulation of DAG-mediated signaling by DGKs (8, 9, 18, 21–23). With anti-CD3 antibody at a suboptimal concentration, we stimulated T cells from mice with varying numbers of alleles of *Dgka* and *Dgkz* and measured the extent of ERK phosphorylation by flow cytometry. This experiment enabled us not only to determine which isoform had greater control over ERK phosphorylation but also to quantify the relative magnitude of DGKα- and DGKζ-mediated suppression of ERK phosphorylation. Loss of DGKζ resulted in a large increase in the percentage of cells with phosphorylated ERK (pERK), whereas loss of DGKα resulted in a consistently lower increase in the percentage of $CD4^+$ and $CD8^+$ T cells with pERK (Fig. 2, A to D).

To analyze the allelic series statistically, we applied a multiple linear regression model with the number of DGKα and DGKζ alleles removed as predictors and the natural log of the percentage of $pERK^+$ positive cells as the dependent variable (Table 1). Because mice with complete deletion of both *Dgka* and *Dgkz* have a severe block in thymic development (22), we eliminated these mice from our analysis. According to the regression model, deletions of *Dgka* and *Dgkz* alleles were statistically significant predictors of the percentage of $pERK^+$ cells for both $CD4^+$ and $CD8^+$ T cells. Deletion of either *Dgka* or *Dgkz* statistically significantly increased the extent of ERK phosphorylation in $CD4^+$ and $CD8^+$ T cells (Table 1), consistent with previous reports (8, 9, 21). However, the magnitude of the effect of deletion of *Dgkz* was greater than that of *Dgka*, with 2.6- and 3.3-fold greater effects of *Dgkz* deletion than of *Dgka* deletion on the natural log of the percentage of $pERK^+$ cells in $CD4^+$ and $CD8^+$ T cells, respectively. We also obtained similar results with Western blotting analysis of purified T cells that were stimulated by antibody-mediated cross-linking of CD3, CD4, and CD28 (fig. S2). The increased ERK phosphorylation observed in DGKζ-deficient T cells compared to that in T cells from the other mice was not a result of the higher percentage of $CD44^{hi}CD8^+$ activated splenic T cells (21), because the percentage of $pERK^+$ cells was similar between the $CD44^{hi}$ and $CD44^{lo}$ populations, regardless of genotype (fig. S3). In addition, the increase in ERK phosphorylation in DGKα- and DGKζ-deficient T cells was dependent on the classical mitogen-activated or extracellular signal–regulated protein kinase kinase (MEK) activation pathway, because treatment with the MEK inhibitor U0126 abrogated ERK phosphorylation after TCR stimulation (fig. S4). Together, these results suggest that DGKζ plays a more dominant role than DGKα in suppressing signals that lead to ERK phosphorylation in $CD4^+$ cells and $CD8^+$ T cells.

DGKζ exhibits greater control than does DGKα over TCR-stimulated phosphorylation of Akt and S6

Simultaneous deletion of *Dgka* and *Dgkz* leads to increased signaling through the Akt pathway, likely as a result of increased Ras-MEK-ERK signaling (7). We therefore tested whether Akt signaling, like that of ERK, was predominantly affected by the deletion of *Dgkz* rather than of *Dgka*. We also examined the phosphorylation of S6 ribosomal protein, an event downstream of both Akt and ERK signaling. At both 5 and 15 min after TCR stimulation, we observed an increase in the percentage of DGKζ-deficient T cells that had pAkt and pS6 compared to that of wild-type T cells (Fig. 3, A and B, top and middle, and C and D). In contrast, and consistent with the more minor role of DGKα in ERK phosphorylation, we observed only a small increase in the percentages of DGKα-deficient T cells that had pAkt and pS6 (Fig. 3). The extent of phosphorylation of the adaptor protein SLP-76 [Src homology 2 (SH2) domain–containing leukocyte protein of 76 kD] was similar among wild-type, DGKα-deficient, and DGKζ-deficient T cells after TCR stimulation (Fig. 3, A and B, bottom panels), indicating that signals proximal to DAG synthesis were unaltered by the deletion of DGKs. Although we observed marked increases (compared to wild-type cells) in the percentages of DGKζ-deficient $CD8^+$ T cells that contained pAkt and pS6, we observed a more modest change in the corresponding percentages of $CD4^+$ T cells. This may be a result of differences in receptor-proximal signaling events, because we also observed less SLP-76 phosphorylation in $CD4^+$ cells compared to that in $CD8^+$ T cells (Fig. 3, A and B, bottom panels), or it may result from the increased proportion with in DGKζ-deficient $CD4^+$ T cells of T_{reg} cells, which are less responsive to TCR stimuli than are conventional $CD4^+$ T cells. This examination of the phosphorylation of ERK, Akt, and S6 demonstrates a consistently more substantial role for DGKζ than for DGKα in suppressing DAG-mediated signaling, particularly signaling downstream of Ras, after TCR engagement. In addition, we observed that T cells deficient in either DGKα or DGKζ had similar increases in the phosphorylation of inhibitor of NF-κBα (IκBα) in response to TCR stimulation (fig. S2), suggesting that the dominant suppressive role of DGKζ did not extend to DAG-mediated activation of protein kinase C-θ (PKC-θ) and its downstream targets.

The relative abundances of DGKα and DGKζ do not explain their differences in function

If the amount of DGKα protein was less than that of DGKζ, genetic deletion of *Dgka* would result in the removal of fewer numbers of DGK molecules and possibly cause more subtle effects on DAG-mediated TCR signaling than would deletion of *Dgkz*. To investigate this possibility, we examined the abundances of DGKα and DGKζ proteins in T cells (fig. S5). Because we lacked the necessary reagents to generate a standard curve from known quantities of pure DGKα and DGKζ proteins, we performed Western blotting analysis of lysates from human embryonic kidney (HEK) 293T cells transfected with plasmids encoding either a fusion of enhanced green fluorescent protein (eGFP) and DGKα (eGFP-DGKα) or eGFP-DGKζ, and generated a standard curve by comparing the band intensities observed by Western blotting analysis with an anti-GFP antibody to those observed by Western blotting analysis with antibodies specific for DGKα or DGKζ. We examined purified wild-type T cells with antibodies specific for DGKα or DGKζ and calculated a GFP intensity equivalent, which enabled us to relate the abundances of the DGKα and DGKζ proteins. Through this

analysis, we found that the amount of DGKα was about threefold greater than that of DGKζ (fig. S5).

The incongruity between the greater protein abundance of DGKα and its relatively weaker role in the suppression of TCR-mediated signaling downstream of Ras suggests that DGKα cannot function redundantly for DGKζ after TCR engagement. To further test this notion, we created bone marrow chimeras by transducing DGKζ-deficient bone marrow cells with retroviruses expressing either wild-type DGKα or wild-type DGKζ and containing an internal ribosomal entry site expressing GFP. In contrast to previous studies (23), this system enables examination of biochemical events in freshly isolated primary cells rather than in cells transduced ex vivo. After hematopoietic reconstitution of the irradiated recipient mice with the transduced cells, we examined ERK, Akt, and S6 phosphorylation after TCR stimulation. Although DGKα was increased in abundance in the transduced cells (fig. S6), we observed no change in ERK, Akt, or S6 phosphorylation in either $CD4^+$ or $CD8^+$ T cells expressing DGKα after TCR engagement (Fig. 4, A and B). In contrast, reexpression of DGKζ substantially suppressed the phosphorylation of ERK, Akt, and S6 after TCR engagement. Together, these results suggest that the relative amounts of DGKα and DGKζ proteins do not explain their differences in function, and that DGKζ has a nonredundant and dominant role in suppressing TCR-dependent Ras signaling.

DGKζ and DGKα localize similarly to the T cell–APC contact site and the immunological synapse, as defined by talin

After TCR stimulation, DAG is synthesized locally at the immunological synapse (6), and translocation of DGK molecules to this T cell–APC contact site could be one mechanism by which DGK function is regulated; thus, we investigated this possibility in primary T cells. We transfected OT-II transgenic TCR, DGKζ-deficient $CD4^+$ T cells with plasmids encoding either eGFP-DGKα or eGFP-DGKζ fusion proteins, incubated the cells with B cells that had been pulsed with OVA peptide, and then allowed T cell–B cell conjugates to form. In unconjugated T cells, both DGKα and DGKζ were diffusely localized throughout the cell, although DGKζ displayed a broader distribution (fig. S7). After formation of the immunological synapse between a T cell and a B cell, both DGKα and DGKζ translocated to the proximal and distal poles of the T cell (Fig. 5A). Through unbiased analysis with an automated MATLAB software script, we quantified the extent of translocation of each DGK isoform by determining the average GFP intensity in sections equivalent to one-third of the cell (those regions being proximal to the immunological synapse, in the middle of the cell, and distal to the immunological synapse) and compared those to the average GFP intensity of the whole cell. Both DGKα and DGKζ exhibited similar and substantial localization to the T cell–APC contact site at 5, 15, and 30 min after conjugate formation, suggesting that the gross localization of DGKα and DGKζ in response to cell conjugate formation was similar (Fig. 5, B and C, and fig. S8 and fig. S9A).

Because DAG synthesis occurs specifically at the immunological synapse (24), we wished to more closely examine the localization of DGK isoforms to this region. We used an automated script to determine the percentage of total cellular GFP that was localized to areas that also contained the cytoskeletal protein talin, which is a marker of the immunological

synapse. We found that DGKα and DGKζ were equally localized to regions containing talin 5 min after cell conjugate formation, whereas a greater percentage of DGKα was localized to talin-containing regions after 15 and 30 min (Fig. 5D and fig. S9B). This greater localization of DGKα than DGKζ at later time points stands in contrast to the lesser role of DGKα in Ras-mediated signaling downstream of the TCR, suggesting the possibility that DGKα has dominant roles in other signaling pathways. Together, these results suggest that DGKα and DGKζ localize at a gross cellular level in similar proportions at the T cell–APC contact site and immunological synapse after the initiation of TCR signaling.

More RasGRP1 associates with DGKζ than with DGKα

Our experimental data suggested that the percentages of total DGKα molecules and DGKζ molecules that localized to the immunological synapse were similar. In addition, our data also suggested that the abundance of DGKζ protein was less than that of DGKα, suggesting that the total number of DGKζ molecules that localized to the immunological synapse after TCR engagement was fewer than the total number of DGKα molecules that were recruited there. The dichotomy of having a fewer number of DGKζ molecules near the contact site but of them having a greater role in TCR signaling potentially could be reconciled by differential binding of the DGK isoforms to DAG-activated RasGRP1. The association of DGKs with RasGRP molecules may enable DGKs to regulate RasGRP molecules through regulation of spatially local DAG pools (18, 25). In transfected HEK 293T cells, DGKζ coimmunoprecipitates with RasGRP1 (26). One possibility, therefore, is that DGKα does not associate with RasGRP1 with the same affinity that DGKζ does. To test this idea, we transfected control HEK 293T cells, eGFP-DGKα–expressing HEK 293T cells, and eGFP-DGKζ–expressing HEK 293T cells with plasmid encoding RasGRP1 and then subjected the cell lysates to coimmunoprecipitations with an anti-GFP antibody (Fig. 6A). We consistently observed that more RasGRP1 coimmunoprecipitated with eGFP-DGKζ than with eGFP-DGKα, suggesting that RasGRP1 associated more strongly with DGKζ than with DGKα. Unexpectedly, we found that similar amounts of eGFP-DGKα and eGFP-DGKζ coimmunoprecipitated with anti-RasGRP1 antibody (Fig. 6B). This finding could be a result of the additional immunoprecipitation of a lower molecular mass species of RasGRP1 that does not form a complex with DGKα and DGKζ, thereby limiting the detection of differences between RasGRP1-DGKα and RasGRP1-DGKζ associations. Overall, these results suggest that the extent of binding of RasGRP1 to DGKζ is at most about threefold greater than that to DGKα.

Modeling suggests that differences in DGK activity, but not in binding affinity to RasGRP1, are sufficient to explain differences in DGK function

Because the differences in the extent of binding of the DGK isoforms to RasGRP1 were not substantial, we wished to determine whether differences in RasGRP1 binding affinity could lead to the disparate functions that we observed. To investigate this question, we used a previously developed mathematical model of Ras activation in T cells (tables S1 and S2 and fig. S10). Previous data suggest that this model correctly predicts the qualitative features of Ras activation kinetics after stimulation of the TCR with various signaling strengths in wild-type and DGKζ-deficient T cells (21, 27). We stimulated wild-type, DGKα-deficient, and DGKζ-deficient splenocytes with increasing concentrations of anti-CD3 antibody in vitro

and then examined ERK phosphorylation as a readout of Ras activation. We observed that, at all concentrations of anti-CD3 antibody, ERK phosphorylation in DGKζ-deficient T cells was more substantial than that in DGKα-deficient T cells (Fig. 7A). We then performed in silico modeling to examine whether differences in the binding of the DGK isoforms to RasGRP1 could lead to our observed experimental results. On the basis of our experimental data of protein abundance and localization at the immunological synapse, we assumed that the abundance of DGKα was threefold greater than that of DGKζ in the system, and that DAG was equally available to both isoforms. As expected, assuming equal catalytic rates and RasGRP1-binding affinities, DGKα-deficient T cells in silico exhibited greater Ras activation at all ranges of TCR stimulus strength than did DGKζ-deficient T cells (Fig. 7B, top left). Surprisingly, when we assumed that the DGK isoforms had equal catalytic rates but that DGKζ had a threefold greater binding affinity for RasGRP1 than that of DGKα, DGKα-deficient T cells still exhibited greater Ras activation than did DGKζ-deficient T cells, which suggested that differences in RasGRP1-binding alone do not lead to changes in DGK isoform function (Fig. 7B, bottom left).

We speculated that differences in the abilities of DGKα and DGKζ to metabolize DAG might explain why a fewer number of DGKζ molecules would have more of an effect on TCR signaling than a larger number of DGKα molecules. In support of this notion, when we assumed that DGKζ had a greater catalytic rate than that of DGKα, but that both DGK isoforms had equivalent RasGRP1-binding affinities, our model predicted that DGKζ-deficient T cells would exhibit greater Ras activation than would DGKα-deficient T cells, which was consistent with our experimental data (Fig. 7B, top right). An increased RasGRP1 binding affinity appeared to enhance differences in Ras activation between DGKα- and DGKζ-deficient T cells only under conditions in which the catalytic rate of DGKζ was increased (Fig. 7B, bottom right). Together, these modeling data suggest that differences in binding affinity to RasGRP1 alone are not sufficient to account for the differences in DGK function, and that differences in DGK catalytic activity are critical to drive the dominant role of DGKζ in suppressing Ras-mediated signaling.

In response to TCR stimulation, the effective enzymatic activity of DGKζ is greater than that of DGKα

To test the prediction that differences in the catalytic activities of DGKα and DGKζ might underlie the dominant function of DGKζ, we first wished to determine whether kinase activity was required for the ability of DGKζ to suppress TCR signaling, because DGKζ also has a scaffolding role that regulates signaling (28). We created bone marrow chimeras with DGKζ-deficient bone marrow cells expressing either wild-type DGKζ or a kinase-deficient mutant DGKζ and then we evaluated ERK, Akt, and S6 phosphorylation after TCR stimulation. Where as wild-type DGKζ rescued the suppression of ERK, Akt, and S6 phosphorylation in both $CD4^+$ and $CD8^+$ T cells, the kinase-defective mutant DGKζ did not (fig. S11, A to D). These results suggest that suppression of TCR signaling requires the kinase activity of DGKζ rather than its function as a kinase-independent scaffold.

We next tested whether DGKα and DGKζ had different catalytic functions, as was predicted by the in silico model (Fig. 7). Because DGKs may undergo post-translational modifications

after TCR stimulation, measurement of enzymatic activity in vitro is difficult. We therefore investigated the effective enzymatic activities of DGKα and DGKζ as defined by the production of PA in intact cells after stimulation of the TCR. Effective enzymatic activity integrates concentrations of DAG, DGK isoform abundance, and kinase activity into a single parameter. On the basis of the in silico data, we predicted that PA abundance would increase after the stimulation of wild-type T cells; that the TCR-dependent increase in PA abundance in DGKα-deficient T cells would be slightly less than that in wild-type T cells because of the remaining more enzymatically active DGKζ, even though a large total number of DGK molecules were removed; and that PA abundance would be almost unchanged in DGKζ-deficient T cells because, even though a small total number of DGKζ molecules were removed, the remaining DGKα would be less functional than DGKζ. Alternatively, because we previously observed a large increase in Ras-mediated signaling in DGKζ-deficient T cells and only a modest increase in DGKα-deficient T cells compared to that in wild-type cells, one might predict that the extent of PA synthesis would be decreased in DGKζ-deficient cells but not in DGKα-deficient cells, at least with the sensitivity of our assay, which measures whole-cell amounts of PA. We examined PA abundances in cells of each genotype both at baseline and after TCR stimulation. We found an average fold increase in PA of 1.30 in wild-type cells (range, 1.27 to 1.35), 1.31 in DGKα-deficient cells (range, 1.17 to 1.52), and 0.97 in DGKζ-deficient cells (range, 0.80 to 1.04) (Fig. 7C). These data suggest that the predominant role of DGKζ compared to DGKα in suppressing Ras-mediated signaling may be the result of its greater effective enzymatic activity or ability to produce PA after TCR stimulation.

DISCUSSION

Although previous work showed that both DGKα and DGKζ inhibit TCR-mediated signaling and T cell activation, a direct comparison of the roles of these two enzymes had not been reported previously. Here, we demonstrated that DGKζ has functions that are distinct from those of DGKα both in vitro and in vivo. As reported by Schmidt *et al*. (20), we found substantially enhanced development of nT_{reg} cells in DGKζ-deficient mice compared to that in wild-type mice, a phenotype that we did not observe in DGKα-deficient mice. Moreover, DGKζ, but not DGKα, was the predominant suppressor of Ras-mediated signals after TCR engagement. The more prominent role of DGKζ compared to that of DGKα was not because DGKζ was present in greater abundance or exhibited enhanced localization to the T cell–APC contact site compared to DGKα. In addition, whereas more RasGRP1 was associated with DGKζ than with DGKα, in silico studies suggested that RasGRP1 binding alone did not determine differences in DGK function. Rather, our in silico and experimental studies raise the possibility that differences in the effective enzymatic efficiencies of DGKα and DGKζ underlie the relatively greater importance of DGKζ in regulating TCR signaling and T_{reg} cell development.

TCR signals are critical for the development of nT_{reg} cells (29). Increased DAG abundance in particular contributes to the development of nT_{reg} cells because DGKζ-deficient mice have a cell-intrinsic increase in their numbers of thymic T_{reg} cells [Fig. 1A and (20)]. Notably, in contrast to DGKζ-deficient mice, DGKα-deficient mice have no increase in the percentages of thymic T_{reg} cells. We observed a substantial increase in the percentage of

$CD25^+FoxP3^-$ cells (which are enriched in T_{reg} cell precursors) in DGKζ-deficient mice compared to that in wild-type mice, which correlated with increased percentages of thymic T_{reg} cells. Surprisingly, DGKα-deficient mice also had a substantial, albeit reduced, increase in the number of $CD25^+FoxP3^-$ cells, but this increase did not translate into an increase in the percentage of thymic T_{reg} cells. These data suggest that loss of DGKζ increases the extent of nT_{reg} cell development not only through the increased generation of T_{reg} cell precursors but also through modulation of other processes during nT_{reg} cell development.

Differences in signaling phenotypes between T cells deficient in either DGKα or DGKζ could provide further clues about the molecular pathways that control nT_{reg} cell development. There are two possibilities: (i) DGKα and DGKζ regulate the same pathways but with different thresholds that are required for nT_{reg} cell development, or (ii) DGKα and DGKζ regulate separate pathways that differentially control nT_{reg} cell development. Because signaling through ERK contributes to the development of nT_{reg} cells in a dose-dependent manner (20), DGKζ-deficient mice might display increased nT_{reg} development compared to that of DGKα-deficient because of the more prominent role of DGKζ in suppressing ERK signaling (Fig. 2C), leading to an increase in the percentage of developing cells that have ERK signaling above a certain threshold required for the development of nT_{reg} cells. Both DGKα- and DGKζ-deficient T cells exhibited similar increases in the extent of phosphorylation of IκBα (fig. S2), which is also essential for nT_{reg} cell development. Thus, whereas loss of DGKζ increases TCR-mediated signaling through both the ERK and NF-κB pathways (20), loss of DGKα may increase TCR-mediated signaling primarily through NF-κB. Because loss of DGKζ increases the extent of nT_{reg} cell development, whereas loss of DGKα does not, these data suggest that activation of the NF-κB pathway alone is insufficient to increase T_{reg} cell development. Rather, NF-κB and ERK signaling may need to be simultaneously engaged to increase nT_{reg} cell generation.

Because we examined the effect of loss of DGKζ in all tissues in the mice, we cannot exclude the possibility that the T cell–extrinsic effects of DGKζ deficiency, altered T cell development, or both might have led to our observed phenotypes. For example, deficiency in DGKζ in epithelial cells and APCs could lead to alterations in the development of thymocytes, leading to changes in nT_{reg} cell development and an alteration of the TCR repertoire of T cells in the periphery; however, in vitro studies suggest that the increased development of nT_{reg} cells in DGKζ-deficient thymocytes is a T cell–intrinsic phenomenon (20). Nevertheless, future experiments with mice that have T cell–specific and inducible deletion of *Dgkz*, will be necessary to determine whether loss of DGKζ in T cells is specifically responsible for the observed phenotypes.

It is intriguing that loss of DGKζ had a greater effect on T cell function and TCR signaling than did loss of DGKα, despite the greater abundance of DGKα relative to that of DGKζ in T cells. We wondered whether the subcellular localization of DGKα and DGKζ within the T cell could account for the differential effects of DGK isoform loss, because DGKζ, but not DGKα, is thought to localize to the T cell–APC contact site in Jurkat cells (18). Surprisingly, we found that in primary murine T cells, both DGKα and DGKζ displayed sustained localization at the contact site and the immunological synapse at least until 30 min after TCR stimulation. The discrepancy between these findings could be because of

differences between Jurkat cells and primary T cells. For example, in Jurkat cells, DGKζ diffusely localizes to the plasma membrane of the cell (18). In contrast, our data demonstrated that DGKζ primarily localized to the proximal and distal poles of primary T cells (Fig. 5B). We also found that, as a percentage of total GFP-tagged molecules, DGKα and DGKζ grossly localized to similar degrees to the immunological synapse after the initiation of TCR signaling. Consistent with these data, interference with the function of DGKs leads to disruption of DAG accumulation at the immunological synapse, as observed by total internal reflection fluorescence microscopy (TIRF), which suggests that DGKα, DGKζ, or both localize specifically to the immunological synapse (6). Because the abundance of endogenous of DGKα protein is greater than that of DGKζ, the total number of DGKα molecules near the immunological synapse is probably greater than the total number of DGKζ molecules. These data suggest that isoform-specific differences in function are not a result of differences in gross localization. However, differences in localization on a smaller scale cannot be excluded. For example, greater localization of DGKζ than of DGKα to regions in which RasGRP1 is present after TCR engagement by an APC might determine DGK function. More refined imaging with TIRF could help to determine whether DGKα and DGKζ localize to different regions of the immunological synapse and specifically to the site of RasGRP1 localization.

Although we did not observe differences in the localization of the DGK isoforms, we found that the extent of the association between RasGRP1 and DGKζ was slightly greater than, or at least equal to, that between RasGRP1 and DGKα. Studies of DGK isoforms have suggested that specific interaction with target proteins is important for regulating the DAG-mediated activation of these molecules. For example, whereas DGKζ inhibits Ras signaling, its structurally related isoform, DGKi, inhibits Rap1 signaling (25). This difference in function correlates with the ability of DGKζ to associate with RasGRP1, which regulates Ras activation, and the ability of DGKi to associate with RasGRP3, which mediates Rap1 activation. In a similar fashion, an increased ability of DGKζ (relative to that of DGKα) to bind to RasGRP1 may be predicted to mediate its enhanced function in T cells. However, our in silico modeling data suggest that a difference in the binding affinities of DGK isoforms for RasGRP1 alone has no effect on their ability to suppress Ras signaling (Fig. 7C). Rather, differential catalytic activity was necessary for changes in the RasGRP1 binding affinity to have a functional effect. These data suggest that the difference in DGK isoform binding to RasGRP1 does not account for the dominant function of DGKζ in suppression of the Ras pathway, and that the binding affinities of DGKs to downstream DAG-activated molecules are not sufficient on their own to modulate DGK function.

Given that DGKα molecules are likely more abundant than DGKζ molecules in T cells and at the T cell–APC contact site, our in silico studies suggested that to account for the increased Ras activation observed in DGKζ-deficient T cells, DGKζ must have a greater effective catalytic activity than that of DGKα. Our experimental studies suggested differences in effective enzymatic activity as a possible mechanism that correlates with the dominant role of DGKζ in attenuating TCR-mediated signaling downstream of Ras. Direct measurement of the physiologically relevant relative catalytic activities of both DGK isoforms is difficult, because both DGKα and DGKζ undergo posttranslational modifications that regulate their activity in ways that cannot be mimicked rigorously in

vitro. For example, the concentration of cytosolic free Ca^{2+}, phosphatidylserine, and cholesterol affects DGKα function (14, 30–33), and measurement of the local concentration of molecules around DGKα molecules after TCR stimulation is difficult. Phosphorylation of the MARCKS domain of DGKζ may also regulate its catalytic activity (19), and measurement of phosphorylation of this specific site in the subset of DGKζ molecules at the immunological synapse after TCR engagement is similarly complicated. We therefore investigated the production of PA after TCR stimulation in cells. We observed a reproducible increase in whole-cell PA production in wild-type and DGKα-deficient T cells after TCR stimulation, suggesting that loss of DGKα had little effect on the conversion of DAG to PA. In contrast, the TCR-stimulated increase in PA was largely abrogated in cells deficient in DGKζ, suggesting that DGKζ, rather than DGKα, is the predominant regulator of PA after TCR stimulation.

In the context of the greater suppression by DGKζ compared to that by DGKα of whole-cell PA production after TCR engagement, the lack of a difference between these isoforms in their regulation of NF-κB signaling, in contrast to RasGRP1 signaling, is somewhat surprising. Our in silico studies suggest that differences in DGK binding affinity to RasGRP1 and PKC-θ would not be predicted to lead to differential regulation of the NF-κB and RasGRP1 pathways. However, the localization of DGKα and DGKζ to regions in which RasGRP1 and PKC-θ are present after TCR stimulation is one possible mechanism that could control differential pathway regulation, because the number of DGK isoform molecules involved in the local metabolism of DAG near these effector molecules could be different. For example, at the level of the immunological synapse, DGKα and DGKζ could localize similarly to regions in which PKC-θ is present but localize differently to regions in which RasGRP1 is present. Microscopic studies of the immunological synapse with high spatial and temporal resolution will be necessary to investigate this hypothesis.

A remaining question concerns why the enzymatic function of DGKζ appears to be enhanced compared to that of DGKα after TCR stimulation. For example, is this difference observed in resting, unstimulated T cells, or does TCR-mediated signaling modulate DGK isoform activity? In terms of regulation, TCR and costimulatory signals inhibit DGKα activity in a manner dependent on the adaptor protein SAP (signaling lymphocyte activation molecule-associated protein), as well as Ca^{2+} release and PLC-γ1 activation (30). However, much less is known about regulation of the kinase activity of DGKζ in T cells. Serine–to–aspartic acid phospho-mimetic mutations in the MARCKS domain lead to decreased catalytic activity in vitro, suggesting that phosphorylation of the MARCKS domain by PKCs may suppress the function of DGKζ (19). Whether this same mode of regulation is true in vivo requires further study. Thus, investigation of TCR-mediated regulation of DGK activity could help to decipher why DGKα and DGKζ seem to display different enzymatic functions in vivo.

Our data demonstrated that reexpression of DGKζ, but not overexpression of DGKα, in DGKζ-deficient T cells rescued the suppression of TCR signaling, suggesting that DGKα cannot function redundantly for DGKζ in the suppression of these pathways. However, TCR stimulation of T cells deficient in DGKα led to modest increases in the amounts of phosphorylated ERK, Akt, and S6 compared to those of wild-type cells, suggesting that

DGKα has some effect on these pathways. One possibility that could reconcile these results is that two different pools of DAG mediate activation of the Ras signaling pathway, with a DGKζ-regulated pool potently stimulating RasGRP1 activity, and a DGKα-regulated pool weakly stimulating RasGRP1 activity. DAG species are not homogeneous, because acyl side chains of varying lengths and degrees of saturation may be connected to the glycerol backbone, and specific DAGs may maximally regulate downstream targets, such as PKCs, although this notion is controversial (34, 35). The development of approaches to differentiate between DAG pools in vivo will be required to rigorously test this idea in primary T cells.

Whereas our data reveal functions in which DGKζ has a dominant role, the coexpression of DGKα in T cells begs the question of whether DGKα has dominant roles in other processes. One such process may be the reorientation of the microtubule organizing complex (MTOC) during formation of the immunological synapse. The synthesis of DAG at the immunological synapse closely precedes, and could be sufficient for, reorientation of the MTOC (6). Further investigation in DGKα- and DGKζ-deficient T cells and higher-resolution microscopic analysis of the subcellular localization of DGKα and DGKζ at the immunological synapse could help to decipher the relative roles of these two isoforms in reorientation of the MTOC.

Our results collectively suggest that, unlike DGKα, DGKζ plays an important role in the development of nT_{reg} cells and has a predominant function in TCR-mediated signaling downstream of Ras. Multiple mechanisms may explain these disparities between isoform function, including differences in binding to downstream DAG-activated molecules and in effective enzymatic function. Because DGKs have been suggested as potential targets in cancer immunotherapy (36), defining these clear functions for DGKζ in T cells will help with the development and therapeutic use of isoform-specific inhibitors of DGKs.

MATERIALS AND METHODS

Mice

Mice deficient in *Dgka* or *Dgkz*, were described previously and were backcrossed seven times to C57BL/6 mice (8, 9). Mice with varying number of alleles of *Dgka* and *Dgkz* were generated by crossing mice deficient in *Dgka* or *Dgkz*. DGKα$^{-/-}$ OT-II and DGKz$^{-/-}$ OT-II mice were generated by crossing C57BL/6 OT-II mice to DGKα$^{-/-}$ or DGKζ$^{-/-}$ mice, respectively. All experiments were performed with age-matched mice. Animal maintenance and experimentation were performed in accordance with the Institutional Animal Care and Use Committee at the University of Pennsylvania.

Flow cytometric analysis of ERK, Akt, and S6 phosphorylation

Spleens were isolated from mice, red blood cells were removed with ACK lysis buffer (155 mM ammonium chloride, 10 mM potassium bicarbonate, 1 mM EDTA), and splenocytes were rested for 2 hours in serum-free medium. For experiments examining ERK phosphorylation in an allelic series of DGKα and DGKζ, rested splenocytes were stimulated for 15 min with anti-CD3 antibody (2.5 μg/ml, 500A2) in RPMI. For experiments examining

ERK phosphorylation in the presence of the MEK inhibitor U0126, cells were rested for 30 min in RPMI followed by a 1-hour incubation with 30 μM U0126 or dimethyl sulfoxide (DMSO) as a control. Cells were then stimulated through the TCR in the presence of 30 μM U0126 or DMSO. For experiments examining Akt and S6 phosphorylation in wild-type, DGKα-deficient, or DGKζ-deficient cells, or in splenocytes isolated from bone marrow chimeric mice, rested splenocytes were stimulated for 5 or 15 min with anti-CD3 antibody (2.5 μg/ml, 500A2) in the presence of Live/Dead Aqua (Life Technologies) in phosphate-buffered saline (PBS). We obtained similar results when the cells were stimulated in RPMI. Stimulation was stopped, and cells were fixed by adding 3 ml of 1× BD Phosflow Lyse/Fix buffer and incubating the cells for 10 to 15 min. Cells were washed with fluorescence activated cell sorting (FACS) buffer (PBS with 3% fetal calf serum and 0.01% sodium azide) and incubated with peridinin chlorophyll protein– Cy5.5 (PerCPCy5.5)–conjugated anti-CD4 antibody, phycoerythrin-Cy5.5 (PECy7)–conjugated anti-CD8a antibody, and Alexa Fluor 700–conjugated anti-CD44 antibody to stain cell surface markers. To analyze cells from bone marrow chimeric mice, cells were incubated with Pacific Blue–conjugated anti-CD45.2 antibody, PerCPCy5.5-conjugated anti-CD4 antibody, and PECy7-conjugated anti-CD8a antibody. Cells were then washed, permeabilized in BD Perm/Wash buffer for 30 min, and incubated with rabbit anti-pERK antibody (Cell Signaling, cat no. 9101S) at a 1:100 dilution, PE-conjugated anti-pAkt(S^{473}) antibody (BD Pharmingen) at a 1:5 dilution, and rabbit anti-pS6 antibody (Cell Signaling) at a 1:100 dilution. Finally, cells were washed and then stained with PE- or Alexa Fluor 647–conjugated anti-rabbit antibodies. Flow cytometric analysis was performed with an LSRII flow cytometer (BD Biosciences), and data were analyzed with Flow Jo software (Tree Star).

Flow cytometric analysis of thymi and spleens

Thymi and spleens from wild-type, DGKα-deficient, or DGKζ-deficient mice were freshly isolated, and cells were incubated with antibodies to detect cell surface TCRb, CD4, CD8, CD44, and CD25. Cells were then fixed with FoxP3 fixation/permeabilization buffer (eBioscience) and incubated with anti-FoxP3 antibody (eBioscience) in the presence of FoxP3 staining buffer (eBioscience). Flow cytometry and data analysis were performed as described earlier.

Generation of eGFP-DGKα– and eGFP-DGKζ–transduced HEK 293T cell lines

HEK 293T cells (5×10^6) were seeded on a 10-cm tissue culture plate. On the same day, HEK 293T cells were transfected with the puromycin resistance gene–containing plasmids pK1-eGFP-DGKα or pK1-eGFP-DGKζ together with the ecotropic packaging vectors pCGP and pHIT123 (a gift from W. Pear, Abramson Family Cancer Research Institute, Perelman School of Medicine, University of Pennsylvania) by the calcium phosphate method. The next day, the seeded HEK 293T cells were infected by adding 1 ml of retrovirus-containing supernatant with polybrene at a final concentration of 4 μg/ml and incubated at 37°C. After 72 hours, cells were selected in medium containing puromycin (3 μg/ml). Experiments with these cell lines were performed after at least 72 hours of selection.

Measurement of endogenous DGK protein abundance

HEK 293T cells transduced with viruses expressing eGFP-DGKα or eGFP-DGKζ were lysed, and serial dilutions based on volume were prepared. T cells from wild-type mice were magnetically purified with CD90.2 microbeads (Miltenyi), lysed, and left undiluted or were diluted twofold in 1% NP-40 supplemented with complete protease inhibitor cocktail (Roche Applied Sciences) and phenylmethylsulfonyl fluoride (PMSF). The cell lysates were then subjected to Western blotting analysis with antibodies specific for GFP, DGKα, or DGKζ. Densitometry was used to create a standard curve to relate GFP band intensity to DGKα or DGKζ band intensity, and a linear regression was performed. The DGKα or DGKζ band intensities from samples of wild-type T cells were then used to calculate a GFP intensity equivalent to estimate the relative amounts of DGKα or DGKζ proteins.

Retroviral transduction of bone marrow cells and generation of bone marrow chimeric mice

Eight- to 12-week-old DGKζ-deficient C57BL/6 mice were injected intraperitoneally with 5 mg of 5-fluorouracil. Four days later, cells from femurs, tibias, and hip bones were isolated by mortar and pestle (37). Cells were resuspended at 2×10^6 to 5×10^6 cells/ml in stimulation medium [Iscove's modified Dulbecco's medium supplemented with 15% fetal bovine serum (FBS), interleukin-3 (IL-3) (10 ng/ml), IL-6 (10 ng/ml), and stem cell factor (50 ng/ml)] and were incubated overnight. The next day, cells were harvested and resuspended at 2×10^6 to 5×10^6 cells/ml in fresh stimulation medium and were plated in 3 ml per well of a six-well plate. Cells were infected by adding 1 ml of retrovirus-containing supernatant with polybrene at a final concentration of 4 μg/ml, centrifuging the cells at 1300g for 2 hours, and incubation at 37°C overnight. The next day, cells were reinfected according to the same protocol. Four hours later, cells were injected retro-orbitally into CD45.1 congenically marked recipient mice that had undergone irradiation (9.50 Gy). Mice were maintained on sterile water supplemented with trimethoprim and sulfamethoxazole for 2 to 3 weeks.

Immunoprecipitations

Control HEK 293T cells and HEK 293T cells transduced with retroviruses expressing either eGFP-DGKα or eGFP-DGKζ were grown in 10-cm culture dishes in Dulbecco's modified Eagle's medium supplemented with 10% FBS and antibiotics. These cell lines were then transfected with the pEF6-huRasGRP1-myc/His wild-type plasmid (a gift from J. Roose, Department of Anatomy, University of California, San Francisco) with the calcium phosphate method. Two days later, cells were washed with PBS and lysed in 0.1% Tween 20, 150 mM NaCl, and 25 mM tris-HCl (pH 7.4) supplemented with PMSF and complete protease inhibitor cocktail (Roche Applied Sciences) for 30 min. Lysates were then centrifuged, and supernatants were precleared by incubation with protein A–Sepharose beads for 1 hour at 4°C on a rotating stand. Precleared lysates were divided into three samples that received anti-GFP antibody (1 μl/ml; Abcam, cat. no. Ab290), anti-RasGRP1 antibody (10 μl/ml; H120, Santa Cruz Biotechnology, cat. no. sc-28581), or normal rabbit IgG (5 μl/ml; Santa Cruz Biotechnology, cat. no. sc-2027). Protein A–Sepharose beads were then added, and samples were incubated overnight at 4°C on a rotating stand. The next day,

samples were washed three times with lysis buffer and three times with lysis buffer containing 500 mM NaCl, and then were denatured in SDS sample loading buffer.

Western blotting analysis of DGKα abundance

Splenocytes were isolated from bone marrow chimeric mice, and T cells were purified by magnetic selection with CD90.2 microbeads (Miltenyi). GFP^+ and GFP^- cells were sorted with a FACS Aria flow cytometer (BD Biosciences), and were lysed in 1% NP-40 supplemented with protease inhibitors. Lysates were subjected to Western blotting analysis with anti-DGKα (Santa Cruz Biotechnology, cat. no. sc-271644), anti-GFP (Clontech, cat. no. 632375), or anti–b-tubulin (Cell Signaling, cat. no. 2146S) antibodies according to standard protocols.

Transduction of primary murine T cells

$CD4^+$ T cells from OT-II $DGK\zeta^{-/-}$, mice were isolated with a $CD4^+$ T cell Isolation Kit (Miltenyi) and were stimulated for 24 to 30 hours in 24-well plates coated with anti-CD3 (1 μg/ml, 2C11) and anti-CD28 (5 μg/ml) antibodies in T cell medium (TCM; Iscove's modified Dulbecco's medium supplemented with 10% FBS and antibiotics) supplemented with recombinant human IL-2 (rhIL-2; 50 U/ml) at a concentration of 2×10^6 to 3×10^6 cells/ml. On the same day, HEK 293T cells were transfected with the plasmid pK1-eGFP-DGKα or pK1-eGFP-DGKζ together with the ecotropic packaging vectors pCGP and pHIT123 (a gift from W. Pear, Abramson Family Cancer Research Institute, Perelman School of Medicine, University of Pennsylvania) by the calcium phosphate method. The next day, 1 ml of virus-containing supernatant from the HEK 293T cells was bound to the wells of a 24-well plate that was coated with retronectin (Takara Bio Inc.) according to the manufacturer's instructions by spinning at 1200g for 2 hours at 30°C CD4 T cell blasts were harvested and resuspended at a concentration of 2×10^6 to 3×10^6 cells/ml in TCM supplemented with rhIL-2 (80 U/ml). The virus-coated wells were washed once with PBS, the T cells were divided into aliquots, and a spinfection was performed by centrifugation at 1200g for 2 hours at 30°C. The next day, cells were harvested and replated on a non–retronectin-coated plate. Transduction efficiencies of greater than 30% were routinely achieved.

Conjugation of T cells and APCs

B cells were selected from wild-type mice by magnetic selection with CD 19 microbeads (Miltenyi). The B cells were washed with serum-free RPMI and stained with 1 μM CMTMR [5-(and-6)-(((4-chloromethyl)benzoyl)amino) tetramethylrhodamine; Life Technologies]. B cells were then washed with TCM and divided into two samples. One sample received OVA peptide (323–339, GenScript) at a final concentration of 5 μg/ml, and samples were incubated for 4 hours at 37°C B cells and transduced T cells were harvested, washed once with serum-free RPMI, and resuspended at 6.66×10^6 and 13.33×10^6 cells/ml, respectively, in serum-free RPMI. B cells (75 μl) were added to T cells (75 μl) in a FACS tube, centrifuged at 200g for 2 min, and incubated for 5 to 30 min in a 37°C water bath. After T cell–B cell conjugation had occurred, 50 μl of cells was transferred to microscope coverslips coated with poly-L-lysine (Sigma), which were incubated at 37°C for 10 min in a humidity chamber. Cells were then fixed with 4% paraformaldehyde, permeabilized with

0.3% Triton X-100, and blocked with 0.01% saponin and 0.25% fish skin gelatin in PBS. Cells were stained with anti-talin antibody (Sigma, cat. no. T3287) followed by Alexa Fluor 647–conjugated anti-mouse antibody (Life Technologies) as well as Alexa Fluor 488–conjugated anti-GFP antibody (Life Technologies) to enhance the intensity of the GFP signal. Cells were mounted onto slides in ProLong Gold Antifade Reagent with DAPI (Life Technologies). Cell conjugates were selected by observation of a GFP-expressing cell (T cell) next to a CMTMR-labeled cell (B cell). Images were acquired at room temperature with Volocity (Improvision) software and a spinning-disk confocal (UltraView ERS 6, PerkinElmer) microscope (Axiovert200, Carl Zeiss) equipped with an ORCA-ER camera (Hamamatsu Photonics) and a 63× oil-immersion plan achromatic objective with a 1.4 numerical aperture.

Image processing and analysis

Images were processed in Fiji software (38) with the “subtract-background” function and by adjusting the dynamic range on the basis of background intensity. Conjugates in which talin accumulated at the immunological synapse were analyzed with a custom-automated MATLAB script. Briefly, GFP images were flattened and thresholded to create a binary image on the basis of background noise intensity. A line was then drawn overlaying the talin image to rotate the image such that the cell conjugate was oriented vertically. After selecting the top and bottom of the cell, the user divided the GFP image into thirds along the *y* axis, and the average GFP intensity in each third, as well as the average GFP intensity of the whole cell, was calculated. As a control analysis, cells were divided into thirds along the *x* axis to determine whether the presence of the nucleus affected this analysis. GFP was not found to be excluded from the middle third of the cell along the *x* axis with this analysis, regardless of the molecule transduced. In addition, analysis of cells transduced to express GFP alone with this method demonstrated no particular localization of GFP to any third of the cell.

Constructs and cloning

Complementary DNAs (cDNAs) encoding DGKα (a gift from A. DeFranco) and DGKζ (Thermo Scientific, cat. no. MMM1013-9200165) were subcloned into the plasmid pEGFP-C1 (Clontech) or the retroviral vector MIGR1 to transduce bone marrow cells. The cDNAs encoding eGFP-DGKα and eGFP-DGKζ were subcloned into the pK1 retroviral vector (a gift from W. Pear) to generate pK1-eGFP-DGKα and pK1-eGFP-DGKζ, which were used for the transduction of primary murine T cells. The cDNAs encoding wild-type DGKζ or a kinase-deficient mutant DGKζ (a gift from I. Mérida) were subcloned into MIGR1 to transduce bone marrow cells.

Analysis of cellular PA abundance

T cells from wild-type, DGKα$^{-/-}$, or DGKζ$^{-/-}$ mice were isolated by magnetic selection with CD90.2 microbeads (Miltenyi), rested for 2 hours, and then left unstimulated or stimulated for 7.5 min with an anti-CD3 antibody (500A2) in RPMI. Cells were washed once with PBS and immediately lysed by sonication. Protein concentration was determined by bicinchoninic acid assay (BCA, Thermo Scientific). Total cellular PA content was

determined with the Total Phosphatidic Acid Kit (Cayman Chemical, cat. no. 700240) according to the manufacturer's protocol and was normalized to protein concentration as described previously (39).

Statistical analysis

Statistically significant differences between groups of data were analyzed as indicated in the figure legends by *t* tests or one-way ANOVA followed by Tukey's post-test and presented in graphical form as means ± SEM by GraphPad Prism software, with the exception of ratiometric data. Differences between groups of ratiometric data were analyzed with nonparametric statistical methods or by logarithmically transforming data to create a normal distribution followed by parametric *t* tests. Ratiometric data are presented in graphical form as medians with interquartile ranges.

In silico modeling

We used a continuous-time Monte Carlo method or the Gillespie method (40) to solve the master equation associated with the signaling network described in fig. S10 and tables S1 and S2. The simulation method includes copy number fluctuations of signaling molecules, also known as intrinsic noise fluctuations (41), that occur as a result of the random nature of stochastic biochemical reactions. We also included cell-to-cell variations in total protein and lipid abundances because of extrinsic noise fluctuations (41). The extrinsic noise fluctuations were implemented as follows. In each individual cell, the total concentrations of protein or lipid were chosen from uniform distributions with the average values shown in table S2. The upper and lower bounds of a uniform distribution for a specific signaling species were chosen by decreasing and increasing the corresponding average value by a factor of 0.0175 (42). The signaling reactions were simulated in a spatially homogeneous simulation box of size, V = area (4 μm^2) × height (0.02 μm), with two compartments representing the plasma membrane and the adjoining cytosolic region (27). This particular choice of the simulation box size ensured that the system was well mixed. The results shown are from simulations performed on 10,000 in silico "cells." Further details regarding the simulation can be found in previous studies (21, 27). The simulations are carried out by using the software package Stochastic Simulation Compiler (SSC) (43). The codes for the simulations are available at http://planetx.nationwidechildrens.org/~jayajit/.

Supplementary Material

Refer to Web version on PubMed Central for supplementary material.

Acknowledgments

We thank T. Patel for help with image analysis; J. Roose, A. DeFranco, W. Pear, and I. Mérida for sharing reagents; members of the Koretzky, Kambayashi, Behrens, and Nichols laboratories for helpful discussions; and J. Stadanlick and M. Jordan for critical reading of the manuscript.

Funding: J.D. is supported by funding from the Research Institute at Nationwide Children's Hospital and NIH grant AI090115; G.A.K. is supported by funding from the Abramson Family Cancer Research Institute and NIH grant R01AI082292.

REFERENCES AND NOTES

1. Smith-Garvin JE, Koretzky GA, Jordan MS. T cell activation. Annu. Rev. Immunol. 2009; 27:591–619. [PubMed: 19132916]
2. Motto DG, Ross SE, Wu J, Hendricks-Taylor LR, Koretzky GA. Implication of the GRB2-associated phosphoprotein SLP-76 in T cell receptor-mediated interleukin 2 production. J. Exp. Med. 1996; 183:1937–1943. [PubMed: 8666952]
3. Imboden JB, Stobo JD. Transmembrane signalling by the T cell antigen receptor. Perturbation of the T3–antigen receptor complex generates inositol phosphates and releases calcium ions from intracellular stores. J. Exp. Med. 1985; 161:446–456. [PubMed: 3919143]
4. Tognon CE, Kirk HE, Passmore LA, Whitehead IP, Der CJ, Kay RJ. Regulation of RasGRP via a phorbol ester-responsive C1 domain. Mol. Cell. Biol. 1998; 18:6995–7008. [PubMed: 9819387]
5. Coudronniere N, Villalba M, Englund N, Altman A. NF-κB activation induced by T cell receptor/CD28 costimulation is mediated by protein kinase C-θ. Proc. Natl. Acad. Sci. U.S.A. 2000; 97:3394–3399. [PubMed: 10716728]
6. Quann EJ, Merino E, Furuta T, Huse M. Localized diacylglycerol drives the polarization of the microtubule-organizing center in T cells. Nat. Immunol. 2009; 10:627–635. [PubMed: 19430478]
7. Gorentla BK, Wan CK, Zhong XP. Negative regulation of mTOR activation by diacylglycerol kinases. Blood. 2011; 117:4022–4031. [PubMed: 21310925]
8. Zhong XP, Hainey EA, Olenchock BA, Jordan MS, Maltzman JS, Nichols KE, Shen H, Koretzky GA. Enhanced T cell responses due to diacylglycerol kinase ζ deficiency. Nat. Immunol. 2003; 4:882–890. [PubMed: 12883552]
9. Olenchock BA, Guo R, Carpenter JH, Jordan M, Topham MK, Koretzky GA, Zhong XP. Disruption of diacylglycerol metabolism impairs the induction of T cell anergy. Nat. Immunol. 2006; 7:1174–1181. [PubMed: 17028587]
10. Zhong XP, Hainey EA, Olenchock BA, Zhao H, Topham MK, Koretzky GA. Regulation of T cell receptor-induced activation of the Ras-ERK pathway by diacylglycerol kinase ζ. J. Biol. Chem. 2002; 277:31089–31098. [PubMed: 12070163]
11. Shin J, O'Brien TF, Grayson JM, Zhong XP. Differential regulation of primary and memory CD8 T cell immune responses by diacylglycerol kinases. J. Immunol. 2012; 188:2111–2117. [PubMed: 22271650]
12. Takahashi M, Yamamoto T, Sakai H, Sakane F. Calcium negatively regulates an intramolecular interaction between the N-terminal recoverin homology and EF-hand motif domains and the C-terminal C1 and catalytic domains of diacylglycerol kinase α. Biochem. Biophys. Res. Commun. 2012; 423:571–576. [PubMed: 22695121]
13. Yamada K, Sakane F, Matsushima N, Kanoh H. EF-hand motifs of α, β and γ isoforms of diacylglycerol kinase bind calcium with different affinities and conformational changes. Biochem. J. 1997; 321:59–64. [PubMed: 9003401]
14. Sakane F, Yamada K, Imai S, Kanoh H. Porcine 80-kDa diacylglycerol kinase is a calcium-binding and calcium/phospholipid-dependent enzyme and undergoes calcium-dependent translocation. J. Biol. Chem. 1991; 266:7096–7100. [PubMed: 1849900]
15. Jiang Y, Qian W, Hawes JW, Walsh JP. A domain with homology to neuronal calcium sensors is required for calcium-dependent activation of diacylglycerol kinase α. J. Biol. Chem. 2000; 275:34092–34099. [PubMed: 10918059]
16. Sanjuan MA, Pradet-Balade B, Jones DR, Martínez-A C, Stone Jc, Garcia-Sanz JA, Merida I. T cell activation in vivo targets diacylglycerol kinase a to the membrane: A novel mechanism for Ras attenuation. J. Immunol. 2003; 170:2877–2883. [PubMed: 12626538]
17. Santos T, Carrasco S, Jones DR, Mérida I, Eguinoa A. Dynamics of diacylglycerol kinase ζ translocation in living T-cells. Study of the structural domain requirements for translocation and activity. J. Biol. Chem. 2002; 277:30300–30309. [PubMed: 12015310]
18. Gharbi SI, Rincón E, Avila-Flores A, Torres-Ayuso P, Almena M, Cobos MA, Albar JP, Mérida I. Diacylglycerol kinase ζ controls diacylglycerol metabolism at the immune synapse. Mol. Biol. Cell. 2011; 22:4406–4414. [PubMed: 21937721]

19. Luo B, Prescott SM, Topham MK. Protein kinase Ca phosphorylates and negatively regulates diacylglycerol kinase ζ. J. Biol. Chem. 2003; 278:39542–39547. [PubMed: 12890670]
20. Schmidt AM, Zou T, Joshi RP, Leichner TM, Pimentel MA, Sommers CL, Kambayashi T. Diacylglycerol kinase ζ limits the generation of natural regulatory T cells. Sci. Signal. 2013; 6:ra101. [PubMed: 24280042]
21. Riese MJ, Grewal J, Das J, Zou T, Patil V, Chakraborty AK, Koretzky GA. Decreased diacylglycerol metabolism enhances ERK activation and augments $CD8^+$ T cell functional responses. J. Biol. Chem. 2011; 286:5254–5265. [PubMed: 21138839]
22. Guo R, Wan CK, Carpenter JH, Mousallem T, Boustany RMN, Kuan CT, Burks AW, Zhong XP. Synergistic control of T cell development and tumor suppression by diacylglycerol kinase a and ζ. Proc. Natl. Acad. Sci. U.S.A. 2008; 105:11909–11914. [PubMed: 18689679]
23. Zha Y, Marks R, Ho AW, Peterson AC, Janardhan S, Brown I, Praveen K, Stang S, Stone JC, Gajewski TF. T cell anergy is reversed by active Ras and is regulated by diacylglycerol kinase-α. Nat. Immunol. 2006; 7:1166–1173. [PubMed: 17028589]
24. Spitaler M, Emslie E, Wood CD, Cantrell D. Diacylglycerol and protein kinase D localization during T lymphocyte activation. Immunity. 2006; 24:535–546. [PubMed: 16713972]
25. Regier DS, Higbee J, Lund KM, Sakane F, Prescott SM, Topham MK. Diacylglycerol kinase τ regulates Ras guanyl-releasing protein 3 and inhibits Rap1 signaling. Proc. Natl. Acad. Sci. U.S.A. 2005; 102:7595–7600. [PubMed: 15894621]
26. Topham MK, Prescott SM. Diacylglycerol kinase z regulates Ras activation by a novel mechanism. J. Cell Biol. 2001; 152:1135–1143. [PubMed: 11257115]
27. Das J, Ho M, Zikherman J, Govern C, Yang M, Weiss A, Chakraborty AK, Roose JP. Digital signaling and hysteresis characterize Ras activation in lymphoid cells. Cell. 2009; 136:337–351. [PubMed: 19167334]
28. Ard R, Mulatz K, Abramovici H, Maillet JC, Fottinger A, Foley T, Byham MR, Iqbal TA, Yoneda A, Couchman JR, Parks RJ, Gee SH. Diacylglycerol kinase ζ regulates RhoA activation via a kinase-independent scaffolding mechanism. Mol. Biol. Cell. 2012; 23:4008–4019. [PubMed: 22918940]
29. Jordan MS, Boesteanu A, Reed AJ, Petrone AL, Holenbeck AE, Lerman MA, Naji A, Caton AJ. Thymic selection of CD4+CD25+ regulatory T cells induced by an agonist self-peptide. Nat. Immunol. 2001; 2:301–306. [PubMed: 11276200]
30. Baldanzi G, Pighini A, Bettio V, Rainero E, Traini S, Chianale F, Porporato PE, Filigheddu N, Mesturini R, Song S, Schweighoffer T, Patrussi L, Baldari CT, Zhong XP, van Blitterswijk WJ, Sinigaglia F, Nichols KE, Rubio I, Parolini O, Graziani A. SAP-mediated inhibition of diacylglycerol kinase a regulates TCR-induced diacylglycerol signaling. J. Immunol. 2011; 187:5941–5951. [PubMed: 22048771]
31. Sakane F, Kai M, Wada I, Imai S, Kanoh H. The C-terminal part of diacylglycerol kinase a lacking zinc fingers serves as a catalytic domain. Biochem. J. 1996; 318(Pt. 2):583–590. [PubMed: 8809050]
32. Epand RM, Kam A, Bridgelal N, Saiga A, Topham MK. The a isoform of diacyl-glycerol kinase exhibits arachidonoyl specificity with alkylacylglycerol. Biochemistry. 2004; 43:14778–14783. [PubMed: 15544348]
33. Fanani ML, Topham MK, Walsh JP, Epand RM. Lipid modulation of the activity of diacylglycerol kinase α- and ζ-isoforms: Activation by phosphatidylethanolamine and cholesterol. Biochemistry. 2004; 43:14767–14777. [PubMed: 15544347]
34. Sánchez-Piñera P, Micol V, Corbalán-García S, Gómez-Fernández JC. A comparative study of the activation of protein kinase C a by different diacylglycerol isomers. Biochem. J. 1999; 337(Pt. 3): 387–395. [PubMed: 9895281]
35. Hinderliter AK, Dibble AR, Biltonen RL, Sando JJ. Activation of protein kinase C by coexisting diacylglycerol-enriched and diacylglycerol-poor lipid domains. Biochemistry. 1997; 36:6141–6148. [PubMed: 9166785]
36. Riese MJ, Wang LCS, Moon EK, Joshi RP, Ranganathan A, June CH, Koretzky GA, Albelda SM. Enhanced effector responses in activated $CD8^+$ T cells deficient in diacylglycerol kinases. Cancer Res. 2013; 73:3566–3577. [PubMed: 23576561]

37. Lo Celso C, Scadden D. Isolation and transplantation of hematopoietic stem cells (HSCs). J. Vis. Exp. 2007; 2:157. [PubMed: 18830434]

38. Schindelin J, Arganda-Carreras I, Frise E, Kaynig V, Longair M, Pietzsch T, Preibisch S, Rueden C, Saalfeld S, Schmid B, Tinevez JY, White DJ, Hartenstein V, Eliceiri K, Tomancak P, Cardona A. Fiji: An open-source platform for biological-image analysis. Nat. Methods. 2012; 9:676–682. [PubMed: 22743772]

39. Bobrovnikova-Marjon E, Pytel D, Riese MJ, Vaites LP, Singh N, Koretzky GA, Witze ES, Diehl JA. PERK utilizes intrinsic lipid kinase activity to generate phosphatidic acid, mediate Akt activation ,and promote adipocyte differentiation. Mol. Cell. Biol. 2012; 32:2268–2278. [PubMed: 22493067]

40. Gillespie DT. Exact stochastic simulation of coupled chemical reactions. J. Phys. Chem. 1977; 81:2340–2361.

41. Swain PS, Elowitz MB, Siggia ED. Intrinsic and extrinsic contributions to stochasticity in gene expression. Proc. Natl. Acad. Sci. U.S.A. 2002; 99:12795–12800. [PubMed: 12237400]

42. Volfson D, Marciniak J, Blake WJ, Ostroff N, Tsimring LS, Hasty J. Origins of extrinsic variability in eukaryotic gene expression. Nature. 2006; 439:861–864. [PubMed: 16372021]

43. Lis M, Artyomov MN, Devadas S, Chakraborty AK. Efficient stochastic simulation of reaction-diffusion processes via direct compilation. Bioinformatics. 2009; 25:2289–2291. [PubMed: 19578038]

44. Stephens LR, Jackson TR, Hawkins PT. Agonist-stimulated synthesis of phosphatidylinositol(3,4,5)-trisphosphate: A new intracellular signalling system. Biochim. Biophys. Acta. 1993; 1179:27–75. [PubMed: 8399352]

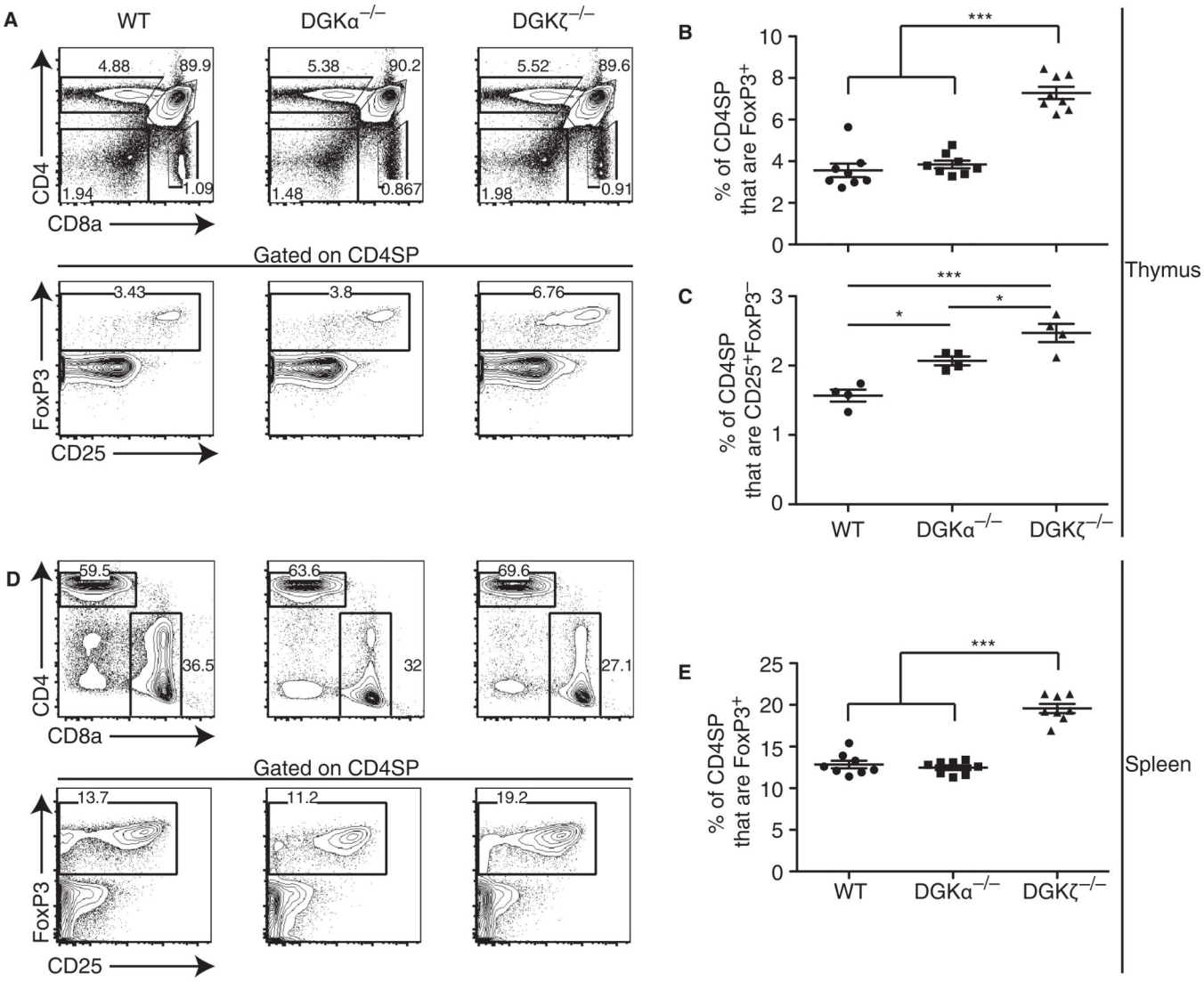

Fig. 1. DGKα-deficient mice, unlike DGKζ-deficient mice, exhibit no increase in the percentage of T_{reg} cells but have increased numbers of T_{reg} cell precursors

(**A**) Top: Representative flow cytometric profiles of freshly isolated thymocytes gated on live singlet cells. Bottom: Gated CD4 SP thymocytes were analyzed for FoxP3 and CD25. Numbers indicate the percentage of cells enclosed within each plot. (**B**) Summary of the percentages of the CD4 SP thymocytes in thymi from the indicated mice that were $FoxP3^+$. (**C**) Summary of the percentages of CD4 SP thymocytes in thymi from the indicated mice that were $CD25^+FoxP3^-$ (enriched for T_{reg} cell precursors). (**D**) Top: Representative flow cytometric profiles of freshly isolated splenocytes from the indicated mice gated on live singlet cells. Bottom: Gated CD4 SP splenocytes from the indicated mice were analyzed for FoxP3 and CD25. (**E**) Summary of the percentages of CD4 SP splenocytes from the indicated mice that were $FoxP3^+$. Data in (B) and (E) are means ± SEM from eight mice of each genotype from a single experiment, and are representative of three independent experiments. Data in (C) are means ± SEM from four mice of each genotype from a single experiment, and are representative of two independent experiments. $*P < 0.05$, $**P < 0.01$,

***$P < 0.001$, as determined by one-way analysis of variance (ANOVA) with Tukey's post-test.

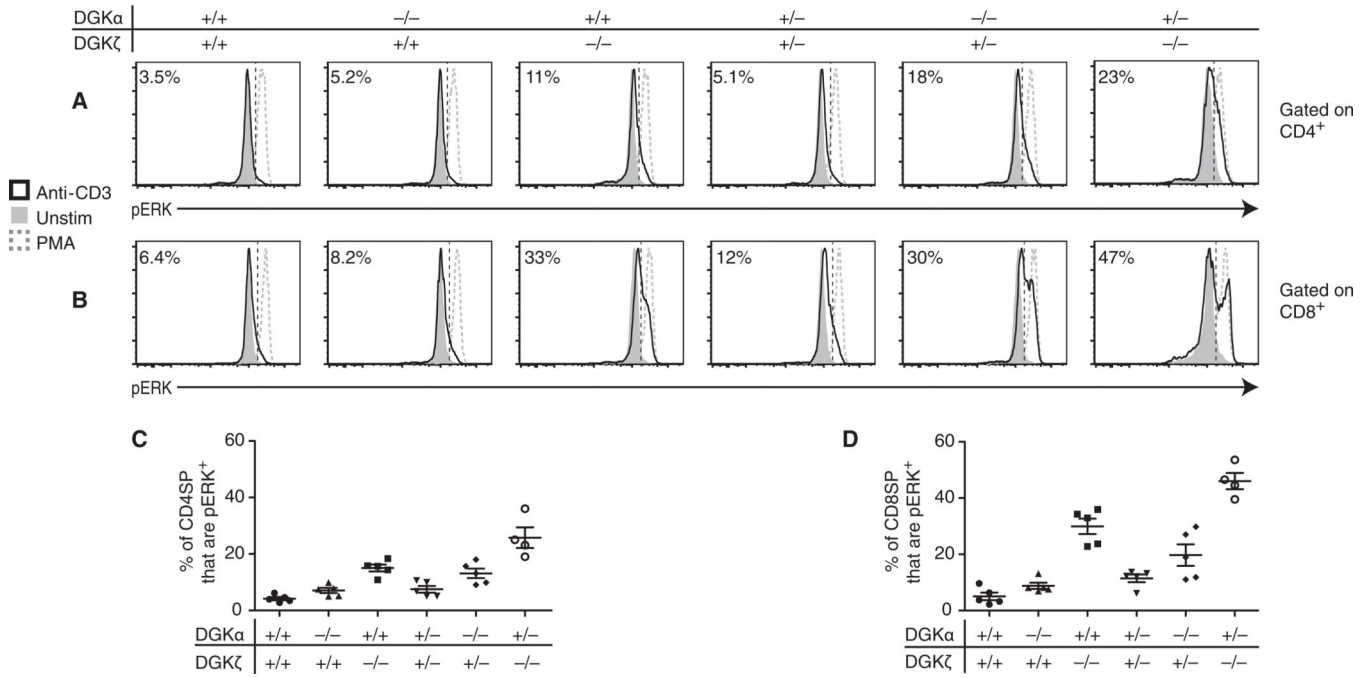

Fig. 2. DGKζ suppresses TCR-dependent ERK phosphorylation to a greater extent than does DGKα

(**A** to **D**) Splenocytes were isolated from wild-type (WT), DGKα$^{-/-}$, and DGKζ$^{-/-}$ mice, rested for 2 hours in serum-free medium, and then stimulated with anti-CD3 antibody for 15 min or with phorbol 12-myristate 13-acetate (PMA; 1 μg/ml) for 15 min, as a positive control. Representative flow cytometric plots of pERK abundance for (A) gated CD4 SP splenocytes and (B) gated CD8 SP splenocytes. Genotypes are indicated at the top. The percentages within each plot indicate the percentage of cells that contained pERK after 15 min of stimulation. The pERK^{+} gate, indicated by the dotted line, was defined on the basis of maximal stimulation of the cells with PMA. Summary of the percentages of (C) CD4 SP splenocytes and (D) CD8 SP splenocytes that contained pERK. For statistical analysis, see Table 1. Data in (C) and (D) are means ± SEM from four to five mice of each genotype from two independent experiments.

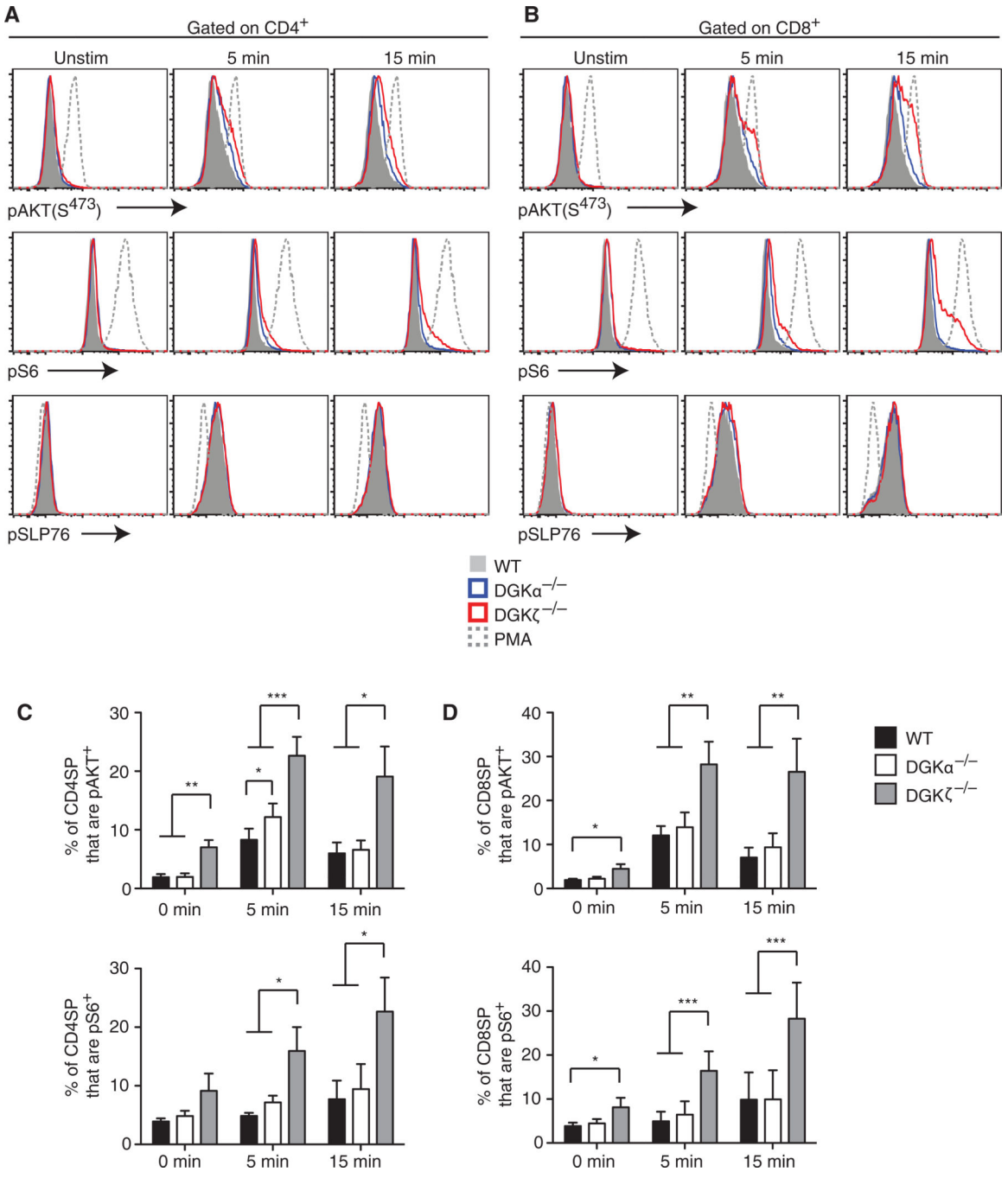

Fig. 3. DGKζ suppresses TCR-dependent phosphorylation of Akt and S6 to a greater extent than does DGKα

(**A** to **D**) Splenocytes were isolated from WT, DGKα$^{-/-}$, and DGKζ$^{-/-}$ mice, rested for 2 hours in serum-free medium, and stimulated with anti-CD3 antibody for 5 or 15 min, or with PMA (1 μg/ml) for 15 min, as a positive control. Representative flow cytometric plots of pSLP76, pAkt(S^{473}), and pS6 in (A) gated CD4 SP splenocytes and (B) CD8 SP splenocytes are shown. Summary of the percentages of (C) CD4 SP splenocytes and (D) CD8 SP splenocytes that contained pAkt and pS6. The gates for the indicated phosphorylated

proteins were defined on the basis of maximal stimulation of cells with PMA. Data in (C) and (D) are means ± SEM from four independent experiments. **P* < 0.05, ***P* < 0.01, ****P* < 0.001, as determined by repeated-measures ANOVA with Tukey's post-test.

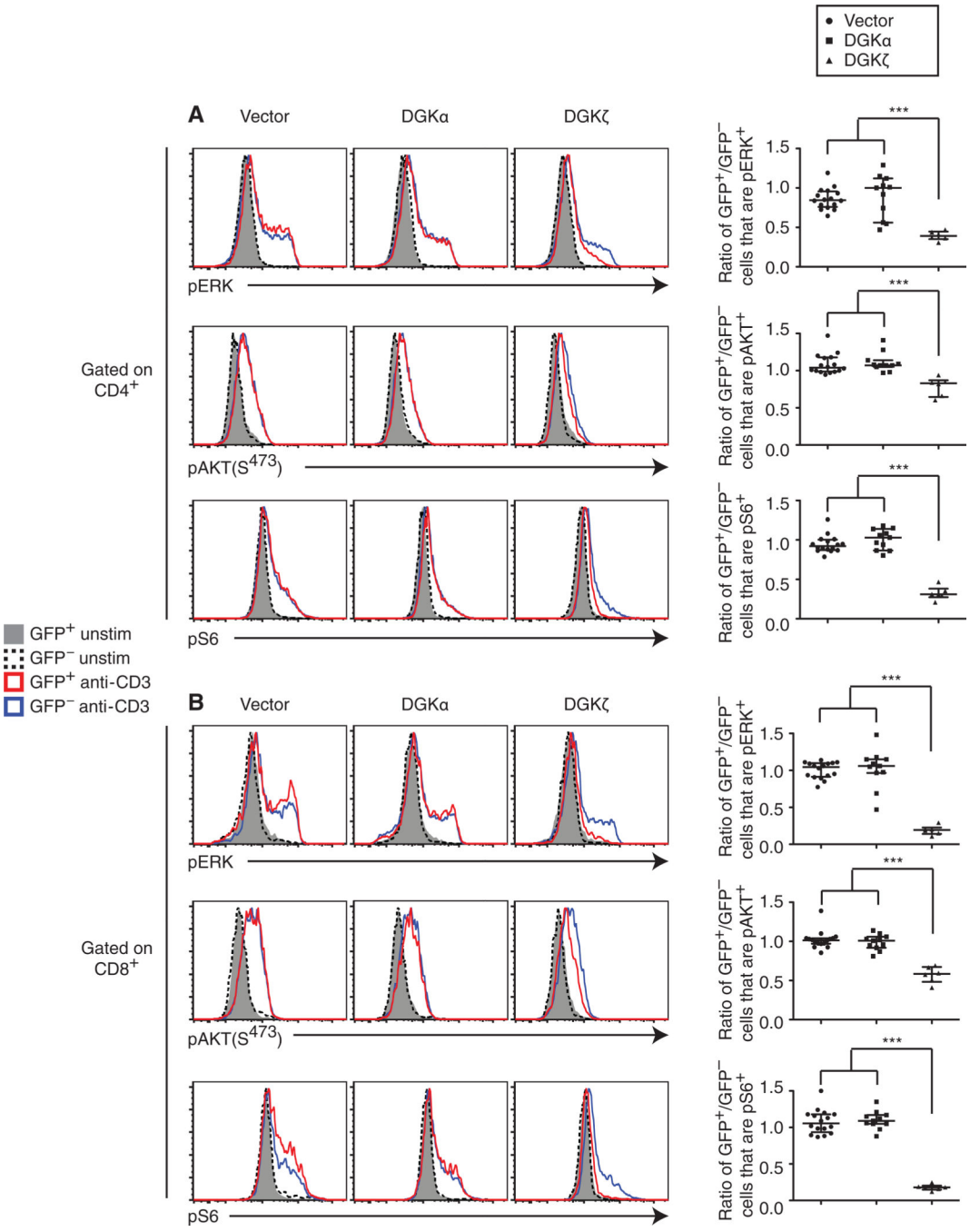

Fig. 4. DGKα and DGKζ do not share redundant functions in suppressing TCR-dependent phosphorylation of ERK, Akt, or S6

(**A** and **B**) CD45.2$^+$DGKζ$^{-/-}$ bone marrow cells were transduced with empty virus (Vector) or with viruses encoding DGKα or DGKζ and then were transferred into CD45.1$^+$ irradiated host mice. After hematopoietic reconstitution, splenocytes were isolated and stimulated with an anti-CD3 antibody for 15 min. Left: Representative flow cytometric plots of pERK, pAkt, and pS6 in cells that were gated on (A) CD45.2$^+$CD4$^+$ or (B) CD45.2$^+$CD8$^+$ and then were gated as GFP$^+$ or GFP$^-$, as indicated. Right: Ratios of the percentages of GFP$^+$ to GFP$^-$

cells that were positive for pERK, pAkt, and pS6 among (A) $CD45.2^+CD4^+$ cells and (B) $CD45.2^+CD8^+$ cells. Ratios of 1 and <1 correspond to there being similar or less phosphoprotein-containing cells in transduced versus nontransduced cells, respectively. The gates for the indicated phosphorylated proteins were defined on the basis of maximal stimulation of cells with PMA. Data are medians with interquartile range from at least five mice for each genotype from two independent experiments. ***$P < 0.001$ by one-way ANOVA on log-transformed data with Tukey's post-test.

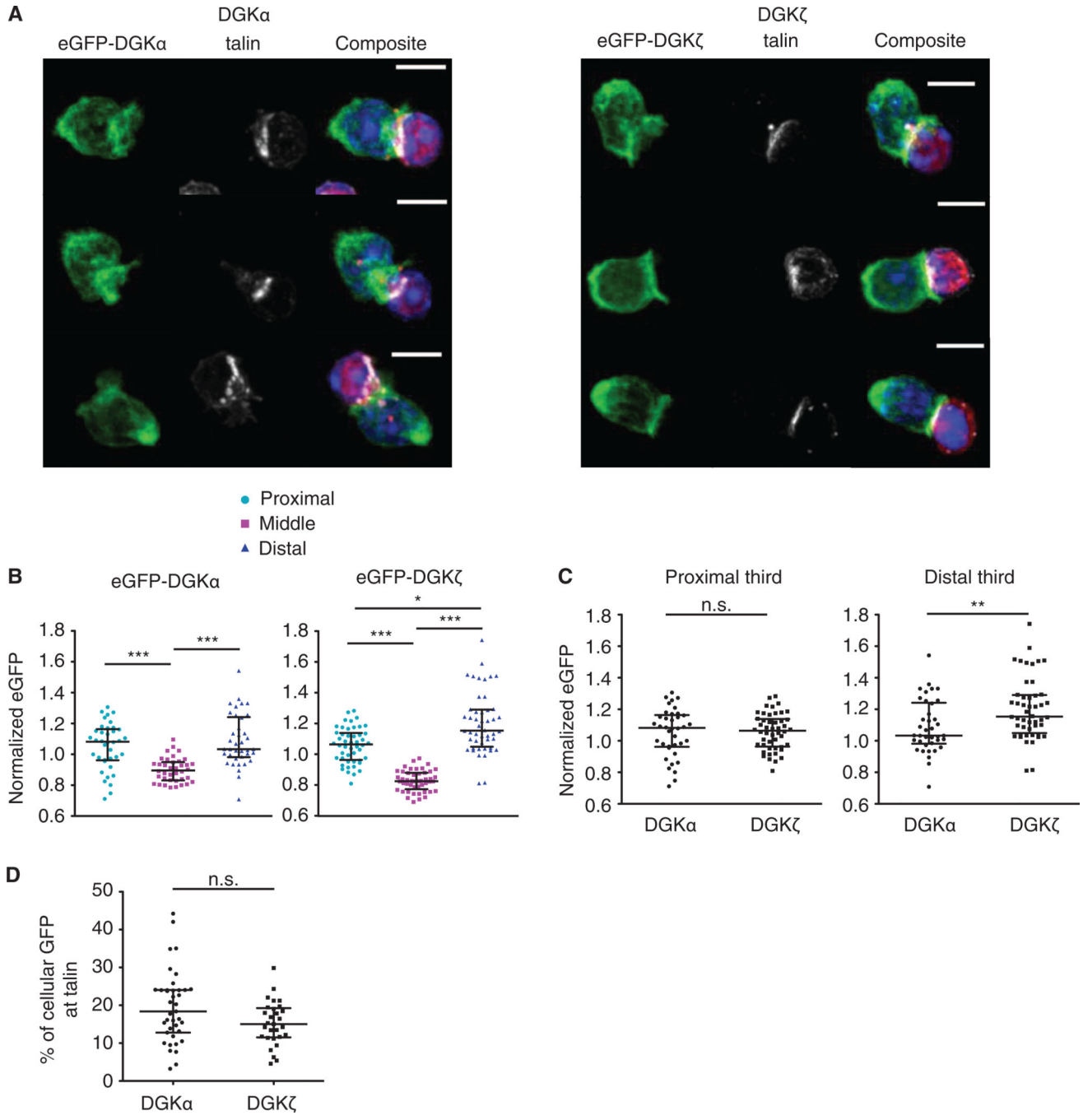

Fig. 5. DGKα and DGKζ localize to similar degrees at the contact site between a T cell and an APC

(**A**) OT-II DGKζ$^{-/-}$ T cells transduced with retroviruses encoding eGFP-DGKα or eGFP-DGKζ were conjugated with ovalbumin (OVA) peptide-pulsed B cells, fixed, and incubated with an anti-talin antibody to mark the immunological synapse. Representative confocal microscopy images captured 5 min after the initiation of cell conjugation are shown. GFP is in green, talin is in white, 4',6-diamidino-2-phenylindole (DAPI; which stains nuclei) is in blue, and CMTMR-labeled B cells are in magenta. Scale bar, 5 μm. (**B**) Ratio of the average

GFP intensity in areas corresponding to one-third of the cell (proximal to the immunological synapse, in the middle of the cell, or distal to the immunological synapse) to the average GFP intensity of the whole cell. Data are from measurements made 5 min after the initiation of conjugation of the indicated T cells. **P*< 0.05, ****P* < 0.001, by Kruskal-Wallis with Dunn's post-test. (**C**) Comparison of the accumulation of eGFP-DGKα and eGFP-DGKζ at the T cell-APC contact sites (proximal third) or the distal poles (distal third) of T cells at 5 min after cell conjugate formation. n.s., not significant. (**D**) Percentages of the total amount of cellular GFP that was localized in talin-containing areas of the indicated T cells. Data are means ± SEM from at least 30 cells for all sets of images from three independent experiments. ***P* < 0.01 by Mann-Whitney test.

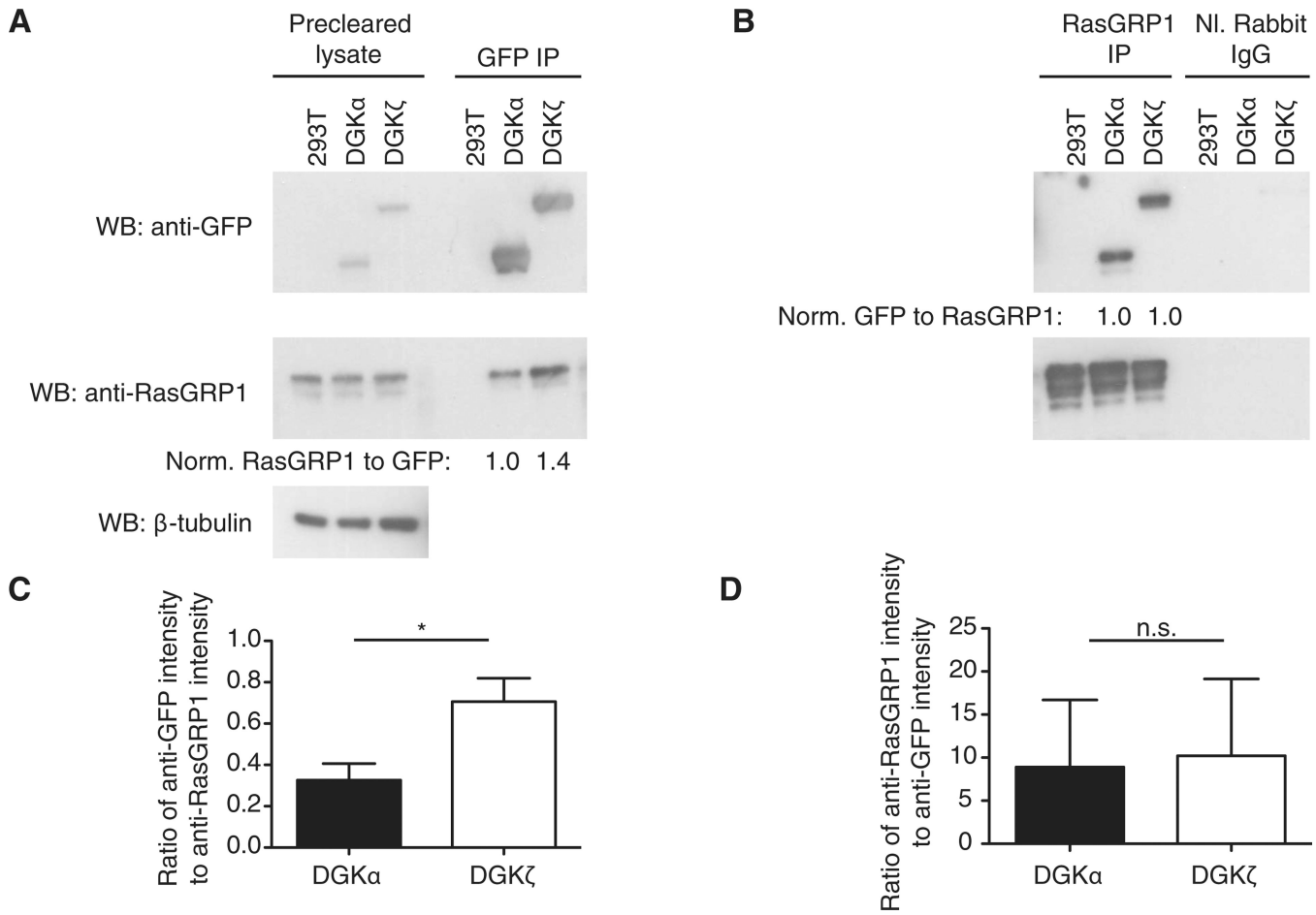

Fig. 6. RasGRP1 associates in greater amounts with DGKζ than with DGKα

(**A** and **B**) Control HEK 293T cells and transduced HEK 293T cells expressing either eGFP-DGKα, or eGFP-DGKζ were transfected with a RasGRP1-expressing plasmid. After 48 hours, cells were lysed, and lysates were divided into three aliquots. (A) Lysates were subjected to immunoprecipitation with an anti-GFP antibody and then were analyzed by Western blotting with anti-GFP or anti-RasGRP1 antibodies. β-Tubulin was used as a loading control. Densitometric analysis was performed to quantify and compare band intensities for the Western blot shown by dividing anti-RasGRP1 staining intensity by anti-GFP staining intensity and normalizing to the ratio for DGKα. (B) Lysates were subjected to immunoprecipitation with an anti-RasGRP1 antibody or with normal rabbit immunoglobulin G (IgG) as a control, and samples were analyzed by Western blotting with anti-GFP and anti-RasGRP1 antibodies. Densitometric analysis was performed to quantify and compare band intensities for the Western blot shown by dividing anti-GFP staining intensity by anti-RasGRP1 staining intensity and normalizing to the ratio for DGKα. (**C**) Ratio of anti-RasGRP1 staining intensity to anti-GFP staining intensity for DGKα and DGKζ for five independent experiments. (**D**) Ratio of anti-GFP staining intensity to anti-RasGRP1 staining intensity for DGKα and DGKζ for four independent experiments. Western blots shown are representative of at least four independent experiments. Data are means ± SEM. **P* < 0.05 by paired *t* test.

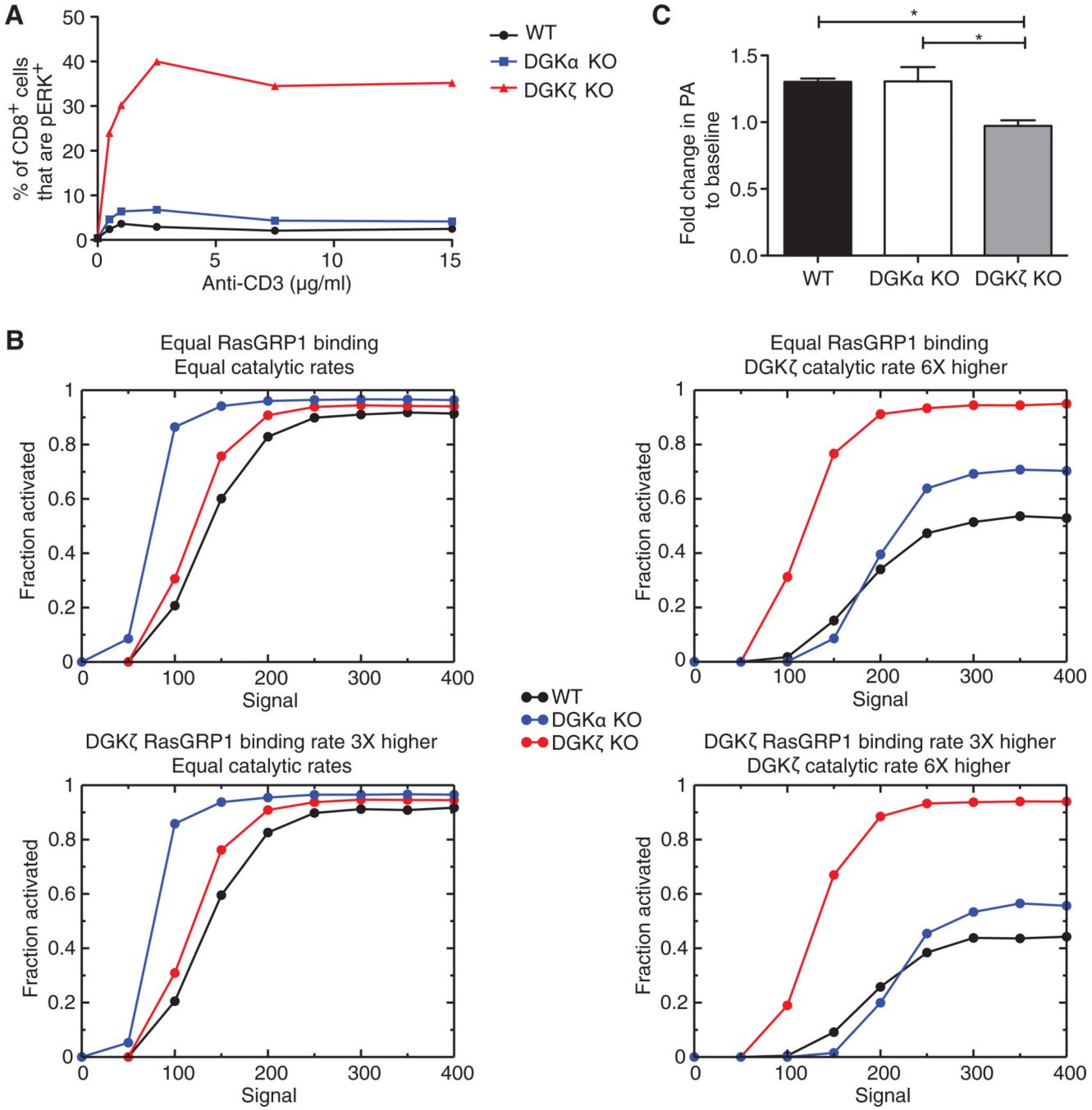

Fig. 7. DGKζ has a greater effective enzymatic activity than that of DGKα in T cells

(**A**) The extent of ERK phosphorylation after 15 min of stimulation of $CD8^+$ T cells isolated from the indicated mice with the indicated concentrations of anti-CD3 antibody was determined by flow cytometry. Data show the percentages $CD8^+$ T cells that contained pERK, and are representative of three independent experiments. (**B**) In silico modeling. The abundance of DGKα, as determined by earlier Western blotting analysis, was assumed to be threefold greater than that of DGKζ. The extent of Ras activation after 15 min of TCR stimulation of WT, $DGK\zeta^{-/-}$, and $DGK\alpha^{-/-}$ T cells was determined by modeling under the

following four conditions: (top left) when the catalytic rates and RasGRP1-binding rates of DGKζ and DGKα were the same; (bottom left) when the RasGRP1-binding rate of DGKζ was assumed to be threefold greater than that of DGKα, and the catalytic rates of DGKζ and DGKα were considered to be the same; (top right) when the catalytic rate of DGKζ was assumed to be sixfold greater than that of DGKα, and the RasGRP1-binding rates of both DGK isoforms were considered equal; and (bottom right) when the RasGRP1 binding rate of DGKζ was assumed to be threefold greater than that of DGKα, and the catalytic rate of DGKζ was sixfold greater than that of DGKα. “Signal” represents the signalosome that is formed after TCRs bind to peptide-MHC-linker of activated T cells (pMHC-LAT) complexes. The concentration of signal qualitatively relates to the concentration of the pMHC-TCR-LAT signalosome; therefore, larger concentrations of the species signal indicate larger doses of antigen. “Fraction activated” indicates the fraction of cells in which RasGTP concentrations were greater than one-third of the total Ras. (**C**) Measurement of the fold change in PA abundance in the indicated cells stimulated with anti-CD3 antibody for 7.5 min compared to that in unstimulated cells. **P* < 0.05 as determined by one-way ANOVA with Tukey’s post-test on data from three independent experiments.

Table 1

Multiple linear regression analysis of the numbers of *Dgka* and *Dgkz* alleles deleted in predicting the percentage of cells containing pERK

A multilinear regression was performed with the numbers of deleted *Dgka* and *Dgkz* alleles as predictors and the natural log of the percentages of pERK-containing cells as the dependent variable. Data were fit according to the model $z = ax + by + C$, where a and b are coefficients representing the magnitude of the response of the dependent variable z to changes in the independent variables x and y, respectively, and C is a constant representing baseline amounts of the dependent variable. The magnitudes of the coefficients and the statistical significance of the independent variables are shown. According to the regression model, deletions of *Dgka* and *Dgkz* alleles were statistically significant predictors of the percentage of $pERK^+$ cells for both $CD4^+$ and $CD8^+$ T cells ($R^2 = 0.768$, $P = 5.74 \times 10^{-9}$, and $R^2 = 0.811$, $P = 3.98 \times 10^{-10}$, respectively).

Dependent variable	Independent variable	Coefficient ± SE	*P*
Log of the percentage of $CD4^+$ cells that were $pERK^+$	Number of *Dgka* alleles deleted	0.270 ± 0.075	0.00130
	Number of *Dgkz* alleles deleted	0.705 ± 0.077	1.23×10^{-9}
	Constant	1.31 ± 0.13	2.70×10^{-10}
Log of the percentage of $CD8^+$ cells that were $pERK^+$	Number of *Dgka* alleles deleted	0.287 ± 0.089	0.00330
	Number of *Dgkz* alleles deleted	0.958 ± 0.091	6.99×10^{-11}
	Constant	1.44 ± 0.16	1.26×10^{-9}